

**SYNTHESIS AND CHARACTERIZATION OF Fe(II) AND Ni(II)
COMPLEXES WITH QUERCETIN**

MUHAMMAD AZRIN BIN MD YUSOF

**Final Year Project Report Submitted in
Partial Fulfillment of the Requirements for the
Degree of Bachelor of Science (Hons.) Chemistry With Management
in the Faculty of Applied Sciences
Universiti Teknologi MARA**

AUGUST 2022

This Final Year Report Project entitled **“Synthesis and Characterization of Fe(II) and Ni(II) Complexes with Quercetin”** was submitted by Muhammad Azrin Bin Md Yusof, in partial fulfillment of the requirement for a Degree of Bachelor of Science (Hons.) Chemistry, in the Faculty of Applied Science, and was approved by



Puan Rabuyah Ni
Supervisor
B. Sc. (Hons.) Chemistry
Center for Applied Sciences Studies
Universiti Teknologi MARA Cawangan Sarawak
93400 Kota Samarahan
Sarawak



Nurhafizah Binti Mohd Selihin
Project Coordinator
B. Sc. (Hons.) Chemistry
Center for Applied Sciences Studies
Universiti Teknologi MARA
Cawangan Sarawak
93400 Kota Samarahan
Sarawak



Ts. Dr. Siti Kartina Binti Abdul Karim
Head
Center for Applied Sciences Studies
Universiti Teknologi MARA
Cawangan Sarawak
Kampus Kota Samarahan 2
93400 Kota Samarahan
Sarawak

Date: 2 August 2022

ABSTRACT

SYNTHESIS AND CHARACTERIZATION OF Fe(II) AND Ni(II) COMPLEXES WITH QUERCETIN

Quercetin which is one of the flavonoid derivatives has several health-promoting effects on humans, including antioxidant, anticancer, antiviral, antibacterial, neuroprotective, and cardioprotective activities. The biological and pharmacological actions of metal-chelated quercetin are much greater than those of quercetin ligand. Recently, it was shown that flavonoids such as quercetin form high-affinity compounds with transition metal ions such as iron and nickel. This technique is regarded as the primary means of enhancing their efficiency in biological tasks such as radical scavenging. In this study, Fe(II) and Ni(II) complexes with quercetin ligand were synthesized in a ratio of quercetin 2:1 metal and characterized using spectroscopic methods such as UV-Vis and FTIR. Fe(II)-quercetin complex was formed with a dark black colour, whereas Ni(II)-quercetin complex was dark brown. According to UV-Vis spectral data, the band I (cinnamoyl system) of both Fe(II)-quercetin and Ni(II)-quercetin complexes had undergone a bathochromic shift, shifting towards longer wavelengths (lower energy). For FTIR spectroscopy, the $\nu(\text{C}=\text{O})$, $\nu(\text{C}=\text{C})$, $\nu(\text{C}-\text{OH})$, and $\nu(\text{O}-\text{H})$ frequencies in Fe(II)-quercetin and Ni(II)-quercetin complexes were shifted somewhat lower from their original value, but $\nu(\text{C}-\text{O}-\text{C})$ shifted slightly higher. Additional spectrum data for Fe(II)-quercetin and Ni(II)-quercetin were discovered at 519 cm^{-1} and 473 cm^{-1} , respectively, representing the $\nu(\text{M}-\text{O})$ absorbance. Both spectroscopic studies demonstrated the complexation of metal with quercetin through an oxygen atom of hydroxyl and carbonyl groups.

ABSTRAK

SINTESIS DAN PENCIRIAN Fe(II) DAN Ni(II) KOMPLEKS DENGAN KUERSETIN

Kuersetin yang merupakan salah satu terbitan flavonoid, mempunyai beberapa kesan positif terhadap kesihatan manusia, termasuk antioksidan, antikanser, antivirus, antibakteria, neuroprotektif dan kardioprotektif. Tindakan biologi dan farmakologi kuersetin yang digabungkan dengan logam jauh lebih berkesan berbanding tindakan ligan kuersetin sahaja. Baru-baru ini, telah terbukti bahawa flavonoid seperti kuersetin mampu membentuk sebatian yang mempunyai pertalian tinggi dengan ion logam peralihan seperti besi dan nikel. Teknik ini dianggap sebagai cara utama untuk meningkatkan kecekapan kuersetin dalam menjalankan tugas biologi seperti pemusnahan radikal. Dalam kajian ini, kompleks Fe(II) dan Ni(II) dengan ligan kuersetin telah disintesis dalam nisbah kuersetin 2:1 logam dan dicirikan menggunakan kaedah spektroskopi. Kompleks Fe(II)-kuersetin terbentuk dengan warna hitam gelap, manakala kompleks Ni(II)-kuersetin berwarna coklat gelap. Menurut data spektrum UV-Vis, jalur I (sistem cinamoil) bagi kedua-dua kompleks Fe(II)-kuersetin dan Ni(II)-kuersetin telah mengalami pergeseran batokromik, beralih ke arah gelombang yang lebih panjang (tenaga yang lebih rendah). Untuk spektroskopi FTIR, frekuensi $\nu(\text{C}=\text{O})$, $\nu(\text{C}=\text{C})$, $\nu(\text{C}-\text{OH})$, dan $\nu(\text{OH})$ dalam kompleks Fe(II)-kuersetin dan Ni(II)-kuersetin telah dianjakkan sedikit, lebih rendah daripada nilai asalnya, tetapi $\nu(\text{C}-\text{O}-\text{C})$ beralih lebih tinggi sedikit. Data spektrum tambahan untuk Fe(II)-kuersetin dan Ni(II)-kuersetin telah ditemui masing-masing pada 519 cm^{-1} dan 473 cm^{-1} , mewakili penyerapan $\nu(\text{M}-\text{O})$. Kedua-dua kajian spektroskopi telah menunjukkan penggabungan logam dengan kuersetin melalui atom oksigen kumpulan hidroksil dan karbonil.

ACKNOWLEDGEMENT

Thanks to the help and assistance of many individuals, this thesis has finally been completed, and I am grateful to every one of them. First and foremost, I would like to thank Allah S.W.T for granting me wisdom, strength, and good health in the completion of this research, even in the final moments. Next, I would like to express my deepest gratitude to my supervisor, Madam Rabayah Ni, for her guidance and support throughout the project. Her valuable knowledge and expertise impartment to me are highly appreciated. I am highly indebted to my parents, Jamaah Binti Kasim and Md Yusof Bin Nordin, for their continuous support and undying love. Without them, I would not have been able to complete this thesis. Not to forget, a sincere thanks to the laboratory assistants, Siti Hajjah Binti Kassim, Fathymah Binti Tukijo, and Mozzarie Shahrayzam Bin Masidi for their continuous technical support throughout the process of my final year project. Finally, immeasurable appreciation to all concerned persons: Mohammad Affaiq Bin Aini, Nur Adibah Binti Zamri, Rozamarie May Pearl Daim, Siti Hanisha Sophia Binti Samat Haron, Erenena Erricatasha Anak Henry, Azira Binti Bahri, who have willingly offered various forms of assistance and motivation during the duration of this research.

(MUHAMMAD AZRIN BIN MD YUSOF)

TABLE OF CONTENTS

	Page
ABSTRACT	iii
ABSTRAK	iv
ACKNOWLEDGEMENT	iv
TABLE OF CONTENTS	vi
LIST OF FIGURES	viii
LIST OF TABLES	ix
LIST OF ABBREVIATIONS	x
CHAPTER 1 INTRODUCTION	
1.1 Background of Study	1
1.1.1 Flavonoids	1
1.1.2 Metal Complexes	4
1.2 Problem Statement	7
1.3 Significance of Study	8
1.4 Objectives of Study	9
CHAPTER 2 LITERATURE REVIEW	
2.1 Flavonoids	10
2.2 Metal Complexes	13
2.3 Synthesis of Fe(II) and Ni(II) complexes with quercetin	16
2.4 Characterization of Iron(II) and Nickel(II) complexes with quercetin	21
2.4.1 UV-Vis Spectroscopic Study	21
2.4.2 IR Spectroscopic Study	26
2.4.3 Mass Spectroscopy	30
METHODOLOGY	
3.1 Materials	33
3.1.1 Chemicals	33
3.1.2 Apparatus	34
3.2 Methods	35
3.2.1 Synthesis of Fe(II) complex with quercetin	35
3.2.2 Synthesis of Ni(II) complex with quercetin	36
3.2.3 UV-Vis Spectroscopic Study	36
3.2.4 IR Spectroscopic Study	37

RESULTS AND DISCUSSION

4.1	Synthesis of metal complexes with quercetin	38
4.1.1	Synthesis of Fe(II) complex with quercetin.....	38
4.1.2	Synthesis of Ni(II) complex with quercetin.....	39
4.2	Characterization of Fe(II) and Ni(II) complexes with quercetin.....	40
4.2.1	UV-Vis Spectroscopy.....	40
4.2.2	FTIR Spectroscopy.....	44

CONCLUSION AND RECOMMENDATIONS

5.1	Synthesis and characterization of Fe(II) and Ni(II) complexes with quercetin.....	49
5.2	Recommendation.....	51

CITED REFERENCES	52
-------------------------------	----

<i>CURRICULUM VITAE</i>	57
--------------------------------------	----

LIST OF FIGURES

Figure	Caption	Page
1.1	Structure of quercetin	3
1.2	Structures of quercetin and its possible chelating sites with metal complexes	3
1.3	The possible structure of Fe(II)-quercetin and Ni(II)-quercetin complexes	4
2.1	Basic flavonoid structure showing rings A, B and C and the numbering, flavonoids and chalcone chemical structures	11
2.2	The EDX spectrum of the Fe(II)-quercetin	18
2.3	Synthesis of metal(II)-quercetin complexes	21
2.4	UV-Vis spectrum of free quercetin ligand and the Fe(II)-quercetin complex	23
2.5	Structure of quercetin and related UV-VIS absorption bands	26
2.6	The IR spectra of quercetin(A) and Fe(II)-quercetin complex(B)	28
2.7	Full scan mass spectrum of the Fe(II)-quercetin and Ni(II)-quercetin complexes	31
4.1	FTIR data of quercetin, Fe(II)-quercetin and Ni(II)-quercetin complexes in the range of $600-440\text{ cm}^{-1}$	47
4.2	FTIR data of quercetin, Fe(II)-quercetin and Ni(II)-quercetin complexes in the range of $4000 - 600\text{ cm}^{-1}$	48

LIST OF TABLES

Table	Caption	Page
2.1	The elemental analysis data of nickel complex with quercetin	20
2.2	Spectroscopy data in the UV-Vis region of the quercetin (Q) ligand in methanol and metal-quercetin complexes in DMSO	25
2.3	IR spectra of quercetin and Fe(II)-quercetin complex	27
2.4	Infrared spectroscopy data of quercetin and metal(II)-quercetin complexes in KBr pellets	29
2.5	FT-IR spectra of metal(II)-quercetin complexes	30
2.6	The ionic radius, number of d electrons and CFSE of the first transition metals	32
4.1	Spectroscopy data in the UV-Vis region of the quercetin ligand and the Fe(II)-quercetin and Ni(II)-quercetin complexes in ultrapure water	43
4.2	IR spectra of quercetin, Fe(II)-quercetin and Ni(II)-quercetin complexes	46

LIST OF ABBREVIATIONS

Fe	: Iron
Ni	: Nickel
Q	: Quercetin
C	: Carbon
H	: Hydrogen
DMSO	: Dimethyl sulfoxide
NaOH	: Sodium hydroxide
KBr	: Potassium bromide
CFSE	: Crystal field stabilisation energies
UV	: Ultraviolet
UV-Vis	: Ultraviolet-Visible
FT-IR	: Fourier-transform infrared
RNA	: Ribonucleic acid
DNA	: Deoxyribonucleic acid
CoA	: Coenzyme A
PD	: Parkinson's disease
ROS	: Reactive oxygen species
EDX	: Energy-dispersive X-ray
XRD	: X-ray diffraction
ATR	: Attenuated Total Reflectance

CHAPTER 1

INTRODUCTION

1.1 Background of Study

1.1.1 Flavonoids

Flavonoids are major natural compounds having a 2-phenyl chromone as the parent nucleus structure. There are many studies associated with the benefits of flavonoids as antioxidant, anticancer, antiviral, antibacterial, neuroprotective and also cardioprotective (Khater *et al.*, 2019). In addition, they are also able to chelate and bind with other metals, which would enhance and produce unique pharmacological and biological properties of the new complexes formed (Raza *et al.*, 2016). It has been discovered that the formation of flavonoids with metal ions may create bioactive complexes (Yu *et al.*, 2020).

Quercetin is one of the naturally occurring flavonoids categorized under the class of flavonols. Besides possessing strong chelating power with other metals, it also has strong biological and pharmaceutical properties, including antioxidant, antibacterial and antitumor (Raza *et al.*, 2016). The structure of quercetin (3, 3', 4',

5, 7-pentahydroxyflavone) is shown in **Figure 1.1**. Referring to the structure, quercetin has three phenolic rings, which consist of A, B and C rings. Chelation of quercetin with other metals could occur through three available sites which are 3-hydroxy-4-keto group, 5-hydroxy-4-keto group and ortho-dihydroxyl (catechol) groups of the B ring (Raza *et al.*, 2016). Metal chelation depends on the pH, solvent polarity and stoichiometric value between quercetin and metal (Kejık *et al.*, 2021). The UV-vis spectrum provides important information regarding quercetin coordination sites. For instance, when metal(II) ions interact with quercetin at a (metal 2:1 flavonoid) ratio, the absorbance of both bands undergoes a bathochromic shift. The 3-hydroxy and 4-keto groups are the first sites to be engaged in the complexation process because the 3-hydroxy group possesses a more acidic proton. The second metal ion is bound by the 3, 4-dihydroxy groups. Because of the lower proton acidity and steric hindrance generated by the initial complexation, the 5-hydroxy group is not participating (Bukhari *et al.*, 2009). The chelation of quercetin with metal(II) ions via 3-hydroxy and 4-keto groups is illustrated in **Figure 1.2** and **Figure 1.3**. With this kind of chelation, the quercetin-metal complexes are observed to have significant increases in biological and pharmaceutical activities, including antioxidant, antibacterial and anticancer compared to free ligand (Porkodi & Raman, 2018).

In this study, we intend to synthesize the Fe(II) and Ni(II) complexes with quercetin, as little research has been devoted to these complexes. Next, the

characterization of Fe(II) and Ni(II) complexes with quercetin also will be investigated by using UV-Visible and FT-IR methods.

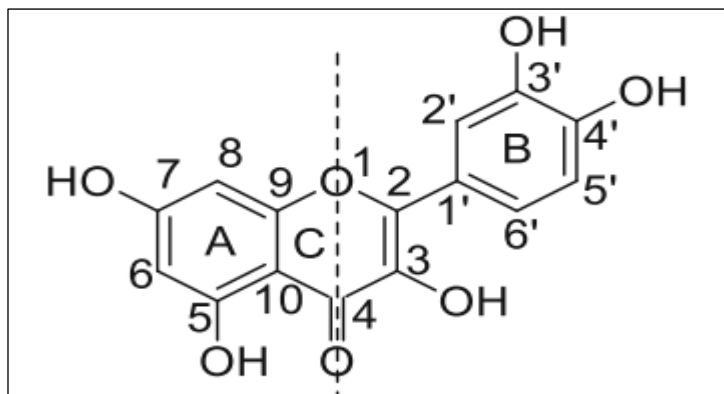


Figure 1.1 Structure of quercetin
Source: Raza *et al.* (2016)

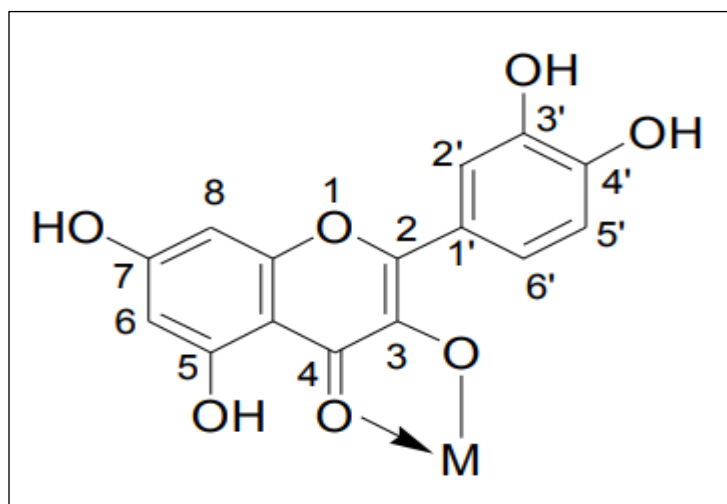


Figure 1.2 Structures of quercetin and its possible chelating sites with metal complexes
Source: Liu & Guo (2015)

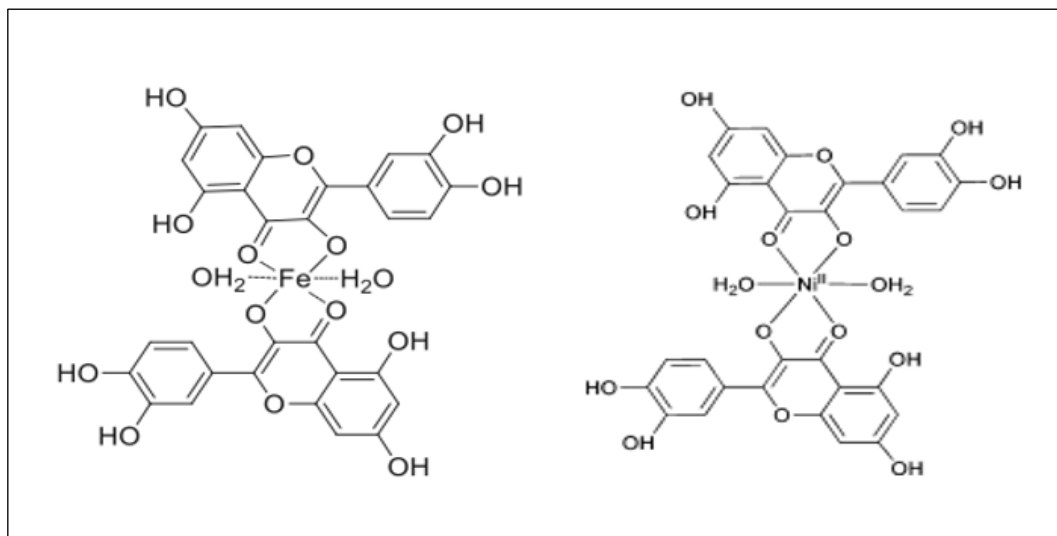


Figure 1.3 The possible structure of Fe(II)-quercetin and Ni(II)-quercetin complexes

Source: Raza *et al.* (2016) ; Tan *et al.* (2009)

1.1.2 Metal Complexes

Iron and nickel have been chosen in this study as there are many biological benefits associated with them. These metals are often consumed as part of a diverse diet or as nutritional supplements, where they serve structural and functional purposes in the human body, including the maintenance of cellular processes engaged in a broad variety of biological activities. It's important to keep metal ion concentrations within an acceptable range, since low quantities may lead to nutritional deficiencies, while excessive ones can cause toxicity (Crans & Kostenkova, 2020).

Firstly, Iron (Fe) is a crucial component in the formation of red blood cells. When it comes to iron in your body, haemoglobin and myoglobin make up around 70 percent of your total iron intake. The oxygen in your blood is carried to your tissues by haemoglobin, which is found in your red blood cells. In muscle cells, myoglobin receives, retains, delivers, and produces oxygen (Gupta, 2014). About 6 percent of the iron in your body is used to make proteins that are important for respiration and energy metabolism, as well as enzymes that make collagen and some neurotransmitters, such as dopamine. Iron is also important for a healthy immune system (Pedro *et al.*, 2019). Besides, all tissues in a young child's growing body need iron. Iron is involved in neuronal myelination from an early age, and is thus found in the brain from birth (Monk *et al.*, 2016).

Nickel (Ni) is a naturally occurring metal that appears in a variety of mineral forms. It is found in every compartment of the environment. Nickel is utilised in a range of metallurgical processes, including electroplating and alloy manufacturing, as well as nickel-cadmium batteries. Additionally, it has excellent function in the biological system and plants (Dixit *et al.*, 2015). Nickel is required for the manufacture of hydrogenases and carbon monoxide dehydrogenases and it is present in a variety of microbial species (Can *et al.*, 2014). Nickel seems to be a critical component of the microflora found in the human gut, where it functions as a cofactor for the enzyme urease. On the other hand, alloys containing nickel, which are often used in jewelry, are known to produce an allergic reaction in around 30%

of women. This application is offset by the addition of Ni-containing alloy implants to heal fractured bones, illustrating the dual nature of nickel as an essential and dangerous metal.

Nickel deficiency inhibits growth, which is especially true during fetal development. Nickel deficiency causes histological and biochemical abnormalities, as well as decreased iron absorption, resulting in anaemia. Additionally, its insufficiency leads to the inhibition of several dehydrogenases and transaminases, affecting glucose metabolism (Kumar & Trivedi, 2016). Nickel is present in the part of the human body where concentrations of nucleic acid (RNA) are abundant and it is believed to be involved in stabilizing the structure of protein (Peter *et al.*, 2015). It may also induce some enzymes to break down glucose. Nickel may have a role in the creation of prolactin, which is necessary for the production of human breast milk. Aside from helping with iron absorption, nickel is involved in the metabolism of adrenaline, glucose, and other hormones, as well as lipids and cell membranes (Peter *et al.*, 2015).

1.2 Problem Statement

Quercetin, a flavonoid derivative possess a number of health-promoting properties in human, including antioxidant, anticancer, antiviral, antibacterial, neuroprotective and cardioprotective effects. Quercetin's beneficial biological features have attracted the attention of pharmaceutical corporations in recent years. Quercetin's weak solubility made it difficult for the body to absorb it, resulting in a low bioavailability in reality. Luckily, this problem could be solved by chelating transition metal ions, such as Fe(II) and Ni(II) with quercetin (Liu & Guo, 2015). On the other hand, the biological and pharmaceutical activities of quercetin with metal chelation are much higher compared to free quercetin ligand (Gençkal *et al.*, 2020). Recently, flavonoids like quercetin were shown to form high-affinity compounds with transition metal ions like iron and nickel (Horniblow *et al.*, 2017). This mechanism is viewed as the major solution to escalating their performance in biological functions such as radical scavenging (Milicevic & Raos, 2016).

Additionally, metal complexes produced by iron binding may have distinct biological properties. For instance, iron chelation affects quercetin's biochemical features such as hydrophilic nature, membrane permeability, and contact with biomolecules (Kejík *et al.*, 2021). In comparison to free quercetin, the metal quercetin complex has increased antioxidant activity as reported by Roy *et al.* (2015). This indicates that metal ions have a major effect on the chemical

characteristics of quercetin. Hence, this research aims to enhance the biological activities of quercetin and help to increase its quality for its application in various sectors especially in the medicinal area. Fe(II) and Ni(II) complexes with quercetin ligand are chosen to be synthesized and characterized in this study.

1.3 Significance of Study

In the medical community, quercetin is regarded as a versatile molecule due to its numerous beneficial effects, including the inhibition of carcinogenesis, the reduction of cardiovascular disease, obesity-related disease, cataracts and neurodegenerative diseases (Kazemipour *et al.*, 2018). Quercetin is a flavonoid that is found in abundance in fruits, leaves, and other plant components. Due to the presence of binding sites within its structure, quercetin may form complexes with a variety of cations, including Fe(II) and Ni(II) (De Castilho *et al.*, 2018).

As the Fe(II) and Ni(II) complexes with quercetin offer a much higher rate of biological and pharmaceutical activities, an attempt was made to synthesize and characterize the complexes. The antioxidant and anticancer capabilities of metal-quercetin complexes have recently attracted a lot of attention since they are more potent than quercetin alone. The Ni(II)-quercetin combination effectively

stimulates plasmid DNA cleavage, resulting in single and double DNA strand breaks. Additionally, the compound exhibited pro-oxidative characteristics and resulted in oxidative DNA damage through the production of reactive oxygen species (Kalinowska *et al.*, 2016). Thus, this research will be beneficial to scientists and chemists in developing new complexes that promote numerous health benefits explained above to the human body shortly.

1.4 Objectives of Study

The specific objectives for this research are:

1. To synthesize Fe(II) and Ni(II) complexes with quercetin.
2. To characterize Fe(II) and Ni(II) complexes with quercetin using spectroscopic methods (UV-Vis, FTIR).

CHAPTER 2

LITERATURE REVIEW

2.1 Flavonoids

Flavonoids or bioflavonoids are a type of secondary metabolites found in plants. The Latin word "flavus" means "yellow," which is their natural colour (Maitera *et al.*, 2018). Their fundamental structure is derived from benzo-pyrone or chromone, and they are low molecular weight polyphenols (Dávila *et al.*, 2018). They provide a range of roles, primarily ecological (by imparting colour to plant parts, particularly flowers and fruits), but also regulate plant development and growth, as well as plant-microbe and plant-animal interactions (Mathesius, 2018). They are engaged in UV protection due to their high antioxidant capabilities. They are heavily debated and investigated due to their beneficial effect on human health.

Flavonoids have a diphenylpropane skeleton, but they are biosynthetically derived from the general phenylpropanoid route, which is reinforced with Malonyl-CoA to generate the final flavonoid main form. Isoflavones are generated when ring B is shifted from position 2 of the ring C to the C atom located in spot 3, while

neoflavonoids are created when ring B is linked in spot 4. On the other hand, ring B remains in position 2 of the basic flavonoid skeleton, which may be classified into subgroups according to the degree of unsaturation and oxidation of ring C (Kejík *et al.*, 2021). These subgroups are shown as in **Figure 2.1**.

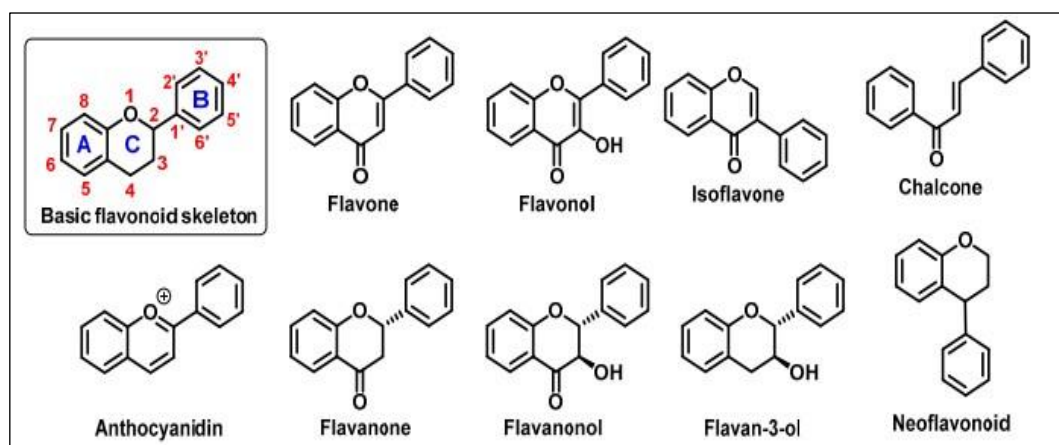


Figure 2.1 Basic flavonoid structure showing rings A, B and C and the numbering, flavonoids and chalcone chemical structures
Source: Kejík *et al.* (2021)

On multiple occasions, it has been said that these substances may be effective in the prevention of a wide range of illnesses. These diseases include cancer, cardiovascular disease, diabetes, and neurological diseases (Grosso *et al.*, 2017). Many studies have shown that flavonoids can fight cancer in different ways. Quercetin, for example, can slow down the activity of a nuclear factor called kappa B and the expression of the P-glycoprotein, which means that angiogenesis, multidrug resistance, and cell migration can be stopped (Singh *et al.*, 2021).

Flavonoid such as quercetin has antihypertensive properties and improves endothelial activities in the treatment of cardiovascular disease (Larson *et al.*, 2012). Hang *et al.* (2018) report that after therapy with bajcalin, individuals with rheumatoid arthritis had lower levels of apolipoproteins, triglycerides, total- and low-density lipoprotein cholesterol, as well as a reduced risk of coronary artery disease. Aboo Bakkar *et al.* (2019) found that taking 235 mg of anthocyanins from *Montmorency cherry* a day helped the body recover endothelium-dependent vasodilation after ischemia-reperfusion injury. In addition, flavonoids have the potential to cure and prevent metabolic disorders. Luna-Vital *et al.* (2018) found that glucosides of cyanidin and delphinidin are powerful inducers of insulin release. Besides, the usage of anthocyanidin-rich extracts has been shown to prevent obesity in normal individuals and to aid in the weight loss of obese patients (Sivamaruthi *et al.*, 2020). Silveira *et al.* (2015) report that regular consumption of red-orange juice raises antioxidant activity in the blood, lowers C-reactive protein and lowers total and low-density lipoprotein cholesterol levels.

Neurodegenerative illnesses are among the many conditions for which flavonoids are being examined closely. Multiple long-term studies have shown a link between regular tea drinking and a reduced risk of Parkinson's disease (PD). Tea contains the antioxidants catechin, epicatechin, and epigallocatechin gallate (Yan *et al.*, 2020). Catechins, like epigallocatechin gallate, have been shown to have a variety of anti-disease Alzheimer's properties (Pervin *et al.*, 2018). Similarly, Fan *et al.*

(2018) publish that people with Parkinson's may benefit from consuming blackcurrant anthocyanins regularly.

Flavonoids' potential to bind strongly with metal ions such as Fe(II) and Ni(II) correlates to their antioxidant capabilities. Chelation occurs in the presence of hydroxyl groups or their carbonyl moiety. Quercetin, a common flavonol, is one of the most studied flavonoids in the world today. Quercetin is a bioactive and abundantly available dietary flavonoid found in the flowers, leaves, and fruits of many plants. However, because of its weak solubility, quercetin is said to be difficult to absorb into the body, resulting in low bioavailability in reality. Luckily, quercetin can form complexes with transition metal ions such as Fe(II) and Ni(II). These metal quercetin complexes demonstrate a wide range of biological properties, including antioxidation, antibacterial activity, antitumor activity, and the capacity to alter a variety of enzymatic functions. Besides, it also could stimulate a new unique pharmacological action (Liu and Guo, 2015).

2.2 Metal Complexes

Iron which is the most common transition metal is a fundamental component of all living organisms. The oxygen supply to the blood is one of the most significant activities of iron. The primary function of iron is to transport oxygen in the

haemoglobin of red blood cells throughout your body, allowing your cells to generate energy. Myoglobin, a protein made from iron, is better at storing and carrying oxygen to the muscle. Besides, there are several enzymes involved in electron transfer and oxidation-reduction processes that need iron to operate properly (Koskenkorva-Frank *et al.*, 2013). Many of their biological roles need the presence of two oxidation states of iron: Fe(II) and Fe(III), which influence their attraction to a variety of biomolecules including amino acids, thiols, phenols and porphyrins. The hem moiety of erythrocyte haemoglobin and muscle myoglobin holds the bulk of the body's iron around 73 percent. The remaining 15% is made up of the so-called iron-labile pool, which is required for a variety of critical ongoing metabolic activities. The rest is kept in cellular ferritin (Kejík *et al.*, 2021).

Iron is required for humankind in the form of haemoglobin and as a complex component of respiration enzymes, especially those that include hemes. Both Fe(II) and Fe(III) chemistry is critical for the binding and function of a large number of different redox proteins, including non-heme proteins. Ligand coordination to iron is critical because it enables redox cycling without involving Fenton chemistry and preventing an uncontrolled ROS formation at the cellular level (Crans & Kostenkova, 2020).

Nickel is one of the most prevalent constituents beneath the Earth in terms of natural abundance. Nickel is found in nature as insoluble particles such as nickel sulphides, oxides, and silicates, which are components of fumes and dusts, or as water-soluble nickel compounds such as nickel acetate, nickel chloride, and nickel sulphate. Nickel's unique physical and chemical properties such as low thermal and electrical conductivities, high corrosion and oxidation resistance, excellent strength and toughness at high temperatures, and the ability to be magnetised make it and its compounds suitable materials for a wide range of applications in commercial industry (Zambelli and Ciurli, 2013). Despite its poisonous potential, nickel is a vital component of living creatures, demonstrating its dual nature as an essential and dangerous metal. In bacteria and lower eukaryotes, nickel is required in the active site of numerous important metallo-enzymes. Nickel deficiency reduces iron absorption from the gut, and the quantities of many metals, including iron, copper, and zinc, in the liver of nickel-depleted animals were similarly reduced. Many enzymes involved in glucose and amino acid metabolism have their particular activity reduced as a consequence of nickel deficiency. Besides, nickel is also believed to have a role in membrane stability and lipid metabolism (Zambelli and Ciurli, 2013).

A number of recent works showed that flavonoids such as quercetin can form high-affinity complexes with transition metal ions, such as iron and nickel. This phenomenon is considered the key mechanism of their biological activity such as

radical scavenging (Milicevic, 2019). Furthermore, metal complexes formed by iron and nickel chelation may display their unique biological activities. This complexation affects their biochemical properties such as lipophilicity, membrane transport, or interactions with biomolecules.

2.3 Synthesis of Fe(II) and Ni(II) complexes with quercetin

Raza *et al.* (2016) demonstrated an experiment to synthesize Fe(II)-quercetin complex by mixing 0.4 mM (0.120 g) of quercetin with 0.2 mM (0.055 g) $\text{FeSO}_4 \cdot 7\text{H}_2\text{O}$. Both the quercetin and $\text{FeSO}_4 \cdot 7\text{H}_2\text{O}$ were pre-dissolved first in 25 mL and 10 mL of methanol respectively before being mixed. Then, the reaction mixture was stirred and refluxed for about 6 hours at a temperature of 60 °C. After being cooled at room temperature, the final product obtained which is the brown colored precipitates was washed with water and methanol. This step was repeated three times to make sure the unreacted $\text{FeSO}_4 \cdot 7\text{H}_2\text{O}$ and quercetin were removed completely. The last step was the vacuum drying of the final product obtained. The percentage yield of Fe(II)-quercetin complex obtained in this study was quite low (64%). The analytically calculated percentage for $\text{C}_{30}\text{H}_{18}\text{FeO}_{14} \cdot 2\text{H}_2\text{O}$ reported was C: 51.90% and H: 3.19%. The yield percentage obtained for $\text{C}_{30}\text{H}_{18}\text{FeO}_{14} \cdot 2\text{H}_2\text{O}$ was quite similar (C: 51.36% and H: 3.31%).

Another experiment was conducted by Papan *et al.* (2020) to synthesize Fe(II)-quercetin complex by adding the quercetin hydrate (0.0050 mole) into 500 mL methanol. This process was carried out at a temperature of 60 °C in a round bottle equipped with an electromagnetic stirrer and a thermometer. The colour change of the mixed solution to yellow indicates that the stirred quercetin hydrate was completely dissolved. Then, 50 % (w/V) of NaOH solution was slowly added to the quercetin hydrate solution to adjust the pH to 12. This process was carried out to alter the protonated quercetin to a deprotonated state. Next, freshly produced Iron(III) chloride (0.0025 mole) in 500 mL ultrapure water was mixed with the deprotonated quercetin solution. After a while, the mixed solution changed colour to dark yellow and was incubated at 60 °C for 2 hours with constant stirring. The dialysis method (MWCO: 12000–14000, Cellu SepT3, USA) was performed on the mixed solution to purify it and then dried with a rotary evaporator. The final product which is the dark powder obtained was then stored in a desiccator at room temperature and kept out of any light. The EDX spectrum of the Fe(II)-quercetin, as shown in **Figure 2.2**, revealed that the compositions of C, O, Na, and Fe were 46.57%, 37.29%, 13.07%, and 3.07%, respectively.

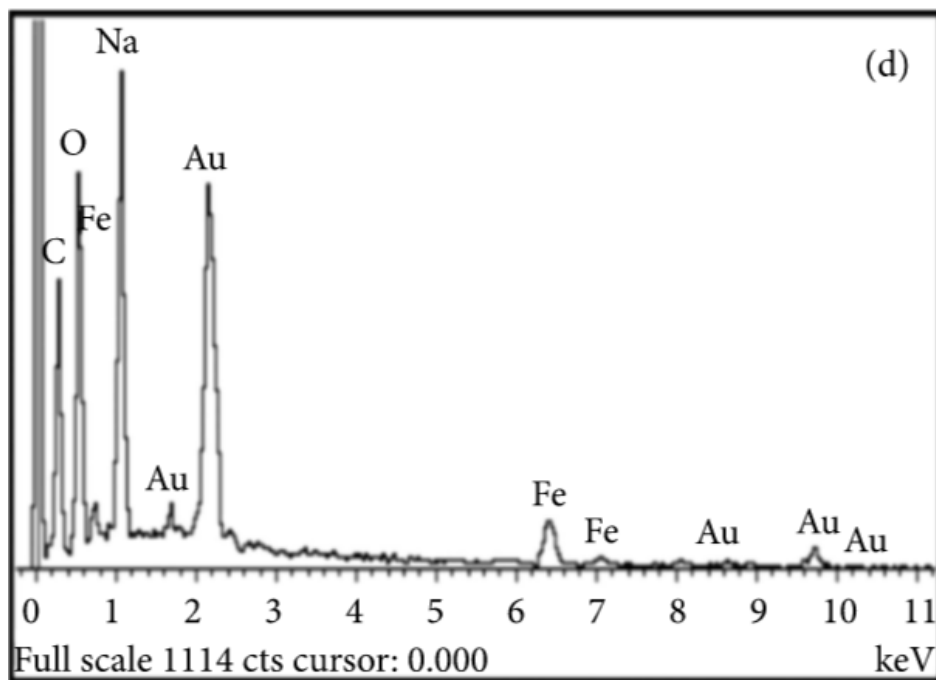


Figure 2.2 The EDX spectrum of the Fe(II)-quercetin
Source: Papan *et al.* (2020)

Trifunsi & Munteanu (2018) synthesized the Fe(II)-quercetin complex by adding the solid quercetin ($C_{15}H_{10}O_7 \cdot 2H_2O$) (0.01 mol) in 20 mL methanol which takes place in the reaction flask. This solution was stirred constantly until the pure quercetin was mixed and dissolved thoroughly. After that, $FeSO_4 \cdot 7H_2O$ (0.0005 mol) was mixed into the solution and stirred for another 2 hours under room temperature. Consequently, the reaction mixture was filtered and evaporated at room temperature. The end product formed which is a dark orange powder was then washed with tert-Butanol to remove the unreacted reagent. The last step of this experiment was the vacuum drying of the final product obtained in a vacuum desiccator. The percentage yield of Fe(II)-quercetin complex and compositions of each element were not stated in this study.

A year later, da Silva *et al.* (2019) synthesized the Ni(II)-quercetin complex by using metal salt, NiCl₂ in a (Ni 1:2 quercetin) stoichiometric ratio with quercetin as the ligand. Then, the metal salt, NiCl₂ which was pre-dissolved in 10 mL of distilled water was mixed with the quercetin binder in 10 mL of methanol. This whole process was carried out using a 50 mL flask under room temperature with continuous stirring. Three drops of trimethylamine then were added to the mixed solution after 20 minutes of reaction followed by the change in colour of the solution instantaneously. For 3 hours, this mixed solution was stirred constantly and kept at a low temperature below 4 °C, refrigerated for two days. This was done to ensure the synthesized Ni(II)-quercetin complex precipitated completely. The last step of this conducted experiment was the filtering of the synthesized compound using a porous plate funnel which was then stored under vacuum conditions in a desiccator. The percentage yield of Ni(II)-quercetin complex and compositions of each element were not stated in this study.

Other than that, Kalinowska *et al.* (2016) also experimented to synthesize the Ni(II)-quercetin complex. The method started with the addition of 0.02 mol of NiCl₂ to the 0.01 mol of quercetin which was pre-dissolved in 20 mL of methanol. Then, NaOH was added to the mixture so that the pH would increase to about 10. The mixture was stirred for 1.5 hours which then resulted in the formation of dark yellow precipitates. The dark yellow precipitates were filtered followed by washing with the mixture of methanol and water in a 3:1 ratio. Lastly, the final product

obtained was dried in a desiccator at room temperature for about 3 days. Based on **Table 2.1**, the elemental analysis carried out in this study reported that the compositions of C, H, and Ni were 42.81 %, 3.03 %, 15.12 %, respectively.

Table 2.1 The elemental analysis data of metal complex with quercetin

Complex	C/%		H/%		Metal/%	
	Exp.	Calc.	Exp.	Calc.	Exp.	Calc.
Na(C ₁₅ H ₉ O ₇).1H ₂ O	51.46	52.59	3.07	3.21	6.78	6.72
Ni(C ₁₅ H ₈ O ₇).2.5H ₂ O	42.81	44.56	3.03	3.22	15.12	14.49

Source: Kalinowska *et al.* (2016)

In another experiment by Shastrala *et al.* (2021), a solution of nickel chloride hexahydrate (NiCl₂.2H₂O) was added to a hot methanolic solution of quercetin in a 50 mL two-necked round bottomed along with the magnetic stirrer. The solution of nickel chloride hexahydrate (NiCl₂.2H₂O) which was pre-dissolved in methanol was added dropwise with continuous stirring and then the mixture obtained was heated under reflux for four to eight hours long. Once done, the end product obtained which was in the solid form was filtered off and washed with diethyl ether followed by drying in vacuum condition. This whole process was summarized in an equation illustrated in **Figure 2.3**. As reported in this study, the Ni(II)-quercetin complex was obtained in good yield which is 80.39%.

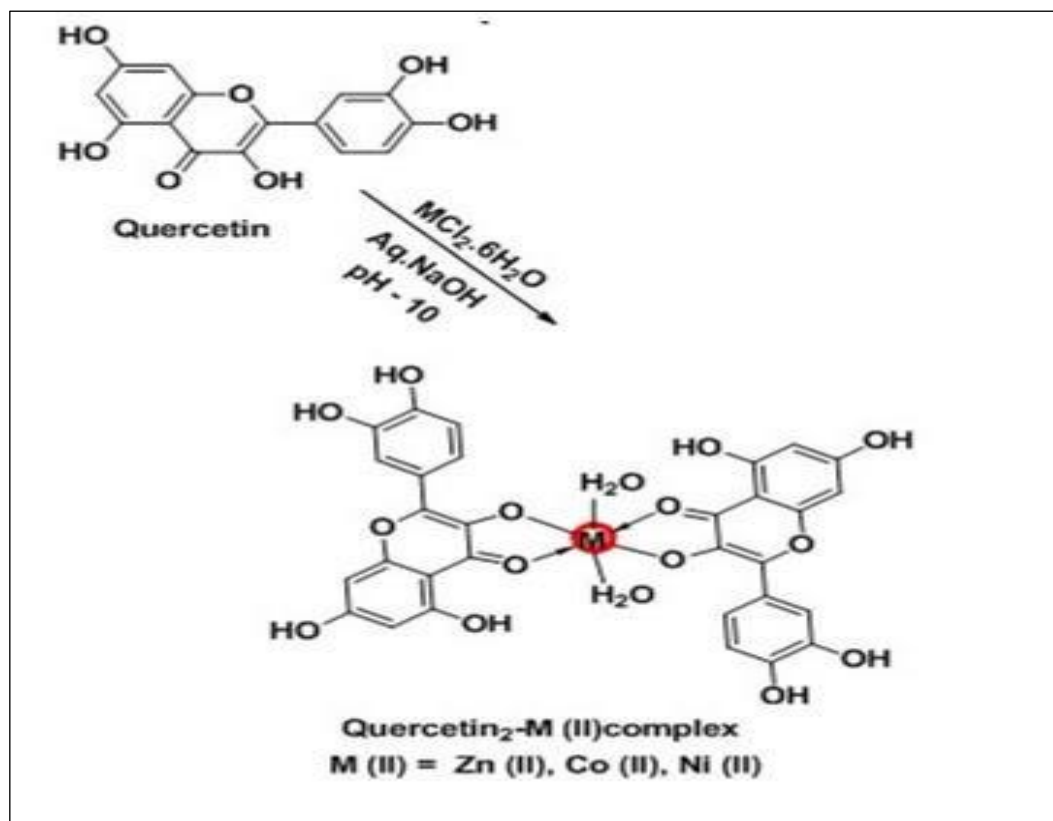


Figure 2.3 Synthesis of metal(II)-quercetin complexes
Source: Shastrala *et al.* (2021)

2.4 Characterization of Iron(II) and Nickel(II) complexes with quercetin

2.4.1 UV-Vis Spectroscopic Study

In an experiment conducted by Raza *et al.* (2016), the comparison of the UV-Vis spectrum of free quercetin ligand and the Fe(II)-quercetin complex were illustrated in **Figure 2.4**. The study found that free quercetin ligand displayed two major absorption bands. The first absorption band was at 372 nm (band I) which represents B-ring absorption (cinnamoyl system). The second absorption band was at 256 nm (band II) which is believed to be related to the absorption of the A-ring

(benzoyl system). Bathochromic shift was detected in the absorbance of both bands when the UV-Vis absorption of the complex was examined. Once $\text{FeSO}_4 \cdot 7\text{H}_2\text{O}$ solution was added to the quercetin methanol solution, and additional peaks at 273 nm (band IV) and 438 nm (band III) appeared which proved a crucial change to the quercetin spectra obtained earlier. It demonstrates that a bathochromic shift of about 17 nm and 66 nm has occurred. The spectral alterations are visible as shown in **Figure 2.4** which indicates the formation of the complex between quercetin and iron has taken place. The newly observed peak at 438 nm in Fe(II)-quercetin complex was due to iron complexation at 3-OH and 4-C=O of quercetin. This hypothesis was concluded as the shift from band II to band IV is rather small. The bathochromic change in the absorbance of both bands, as well as the more acidic nature of the proton of the 3-hydroxy group, explained why the 3-hydroxy and 4-keto groups are the first sites to be implicated in the complexation process. The 5-hydroxy group is not involved because of the lower proton acidity and steric hindrance caused by the initial complexation.

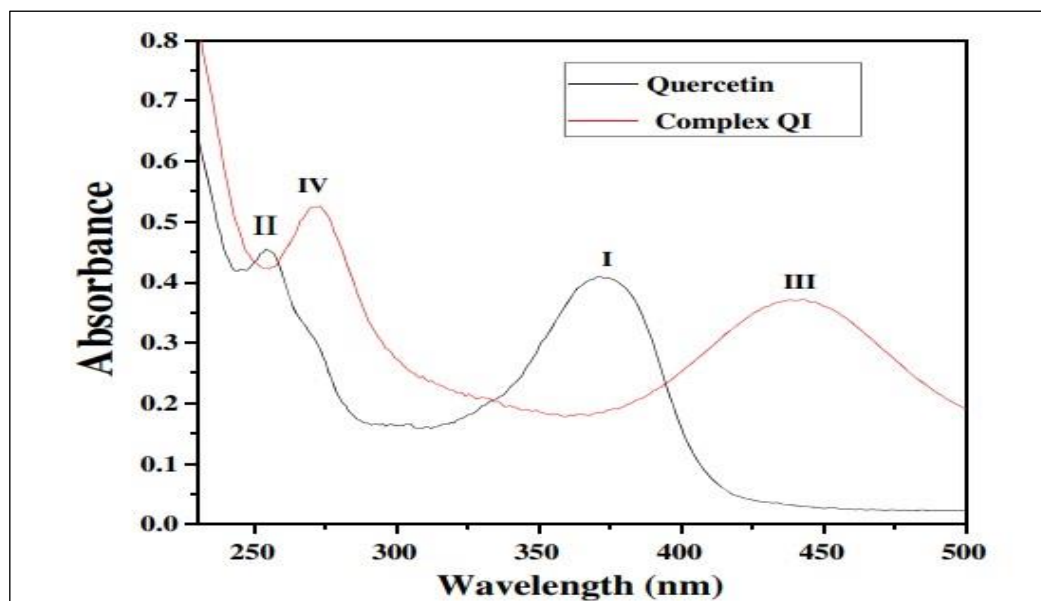


Figure 2.4 UV-Vis spectrum of free quercetin and the Fe(II)-quercetin complex
Source: Raza *et al.* (2016)

Another experiment conducted by da Silva *et al.* (2019) also analysed the spectroscopic measurements of Fe(II) and Ni(II) complexes with quercetin. There were two absorption bands in quercetin's electronic spectrum in methanol, both of which were related to transitions $\pi \rightarrow \pi^*$. Band I was located at 378 nm and represented the conjugated system between the rings B and C (the cinnamoyl system), while band II was located at 260 nm and represented the conjugated system between ring A and carbonyl of ring C (benzoyl system). The electronic spectra of the molecule quercetin still have a band in the 215 nm range ascribed to the electronic transitions of the aromatic ring.

Table 2.2 showed the bathochromic shift in band I which was observed in the electron spectra of Fe(II)-quercetin and Ni(II)-quercetin complexes in dimethyl sulfoxide (DMSO). It explained the interaction of the metal with the 3-hydroxyl

group of quercetin and resulting in an electronic redistribution between the flavonoid molecule and the metal ion, forming an extended π binder system. As the 3-hydroxy group owned more acidic hydrogen, both 3-hydroxy and 4-oxo groups became the initial coordination sites participating in the complexation process and affected the band's displacement (Cherrak *et al.*, 2016). Due to its lower acidity and the spatial obstacle provided by the initial complexation, the hydroxy group positioned in position 5 was not participating in the coordination process.

Following the formation of the complexes Fe(II)-quercetin and Ni(II)-quercetin, band II shifted only around 0-5 nm. On the other hand, band I moved significantly to the red area by approximately 100 nm, indicating the coordination of metal(II)-quercetin through ring C. Cherrak *et al.* (2016) stated that band formation at 438 nm in the electronic spectrum suggested that coordination of metal with the 3-OH group to Fe metal center. It is possible to say that the coordination of the Fe(II) ion with the 3-OH group was also noticed in the electronic spectra of Fe(II)-quercetin at 442 nm. The bands of charge transfer transitions of the metal-binder type were also seen in the same area as band I, which supported the substantial shift.

Table 2.2 Spectroscopy data in the UV-Vis region of the quercetin ligand in methanol and the metal quercetin complexes in DMSO

Compound	Bands (nm)	Band I (nm)	Band II (nm)
Quercetin	378, 260, 215	378	260
Fe(II)-quercetin	256, 379, 442	442	256
Ni(II)-quercetin	256, 348, 449	449	256

Source: da Silva *et al.* (2019)

The next experiment that implement the study on UV-Visible Spectroscopy was done by Trifunshi & Munteanu (2018). UV-Vis spectra in methanol were recorded in the range of 250-800 nm. According to the study, quercetin like the majority of flavonoids had two major absorption bands in the UV-Vis range. The first one was at 372 nm (band I) for B-ring absorption (cinnamoyl system) and the second one was at 256 nm (band II). This was assumed to be related to A ring's absorption (benzoyl system) as shown in **Figure 2.5**. According to this study, bathochromic shifts occurred in the absorbance of both bands I and II due to the reaction of metal(II) ions with quercetin at the ratio of 2:1. For example, bathochromic shifts occurred on Fe(II)-quercetin complex to 280 nm and 410 nm from origin. These alterations aid the coordination of quercetin via 4-oxo and 5-hydroxy groups.

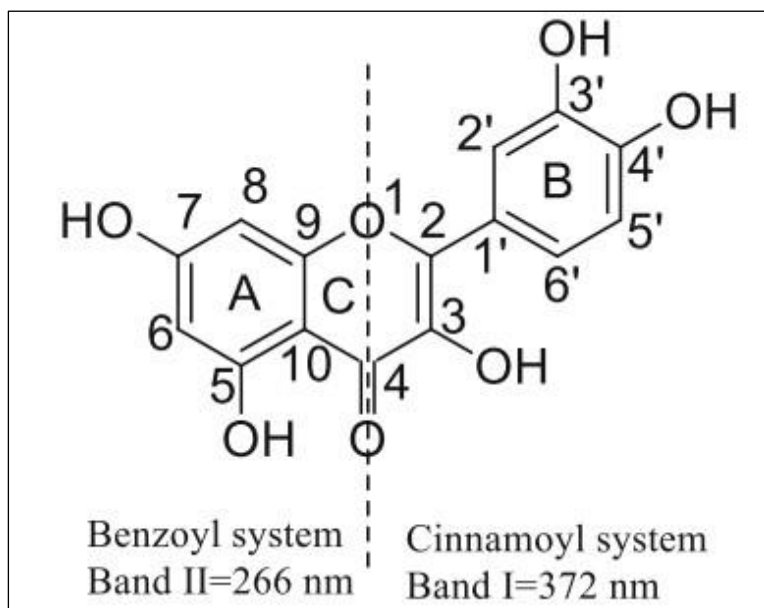


Figure 2.5 Structure of quercetin and related UV-VIS absorption bands
Source : Trifunshi & Munteanu, (2018)

2.4.2 IR Spectroscopic Study

In an experiment conducted by Raza *et al.* (2016), iron-quercetin binding was studied by using KBr pellets with a range of spectral between 4000 and 400 cm^{-1} . One of the main reasons for using Infrared Spectroscopy was to study the binding characteristics as well as the coordination sites of quercetin. The comparative analysis of the infrared spectra of the quercetin molecule and the complexes also indicates the presence of the main bands, with some changes due to the complexation process and metal coordination.

The primary peaks of quercetin and Fe(II)-quercetin complex obtained in this study were shown in **Table 2.3**. By comparing the IR spectra of quercetin and Fe(II)-quercetin complex as shown in **Figure 2.6**, the initial C=O stretching mode of free quercetin ligand at 1661 cm^{-1} was shifted to 1646 cm^{-1} as the result of complex formation. This type of shift proved the coordination of carbonyl oxygen with Fe(II) ion occurred. Furthermore, the initial band located at 1611 cm^{-1} and 1262 cm^{-1} which were related to $\nu(\text{C}=\text{C})$ and $\nu(\text{C}-\text{O}-\text{C})$ frequencies also have slightly shifted to 1594 cm^{-1} and 1277 cm^{-1} respectively in the Fe(II)-quercetin complex. This result indicates an increase in bond order which suggested that metal coordination has occurred. Besides, the formation of the Fe(II)-quercetin complex can be proved by the existence of the Fe-O stretching vibration band at 630 cm^{-1} which cannot be detected in the free quercetin ligand. The existence of water molecule may be the reason for the formation of broad bands for $\nu(\text{OH})$ frequencies of quercetin ($3406\text{--}3323\text{ cm}^{-1}$) and complex Fe(II)-quercetin (3206 cm^{-1}). The stretching $\nu(\text{OH})$ frequency was moved toward lower wavenumber due to the breakdown of the hydrogen bonds in favour of the metal chelation.

Table 2.3 IR spectra of quercetin and Fe(II)-quercetin complex (band position in cm^{-1})

Compound	$\nu(\text{C}=\text{O})$	$\nu(\text{C}=\text{C})$	$\nu(\text{O}-\text{H})$	$\nu(\text{C}-\text{O}-\text{H})$	$\nu(\text{C}-\text{O}-\text{C})$	$\nu(\text{Fe}-\text{O})$
Quercetin	1661	1611	3406-3323	1319	1262	Absent
Fe(II)-quercetin	1646	1594	3206	1356	1277	630

Source: Raza *et al.* (2016)

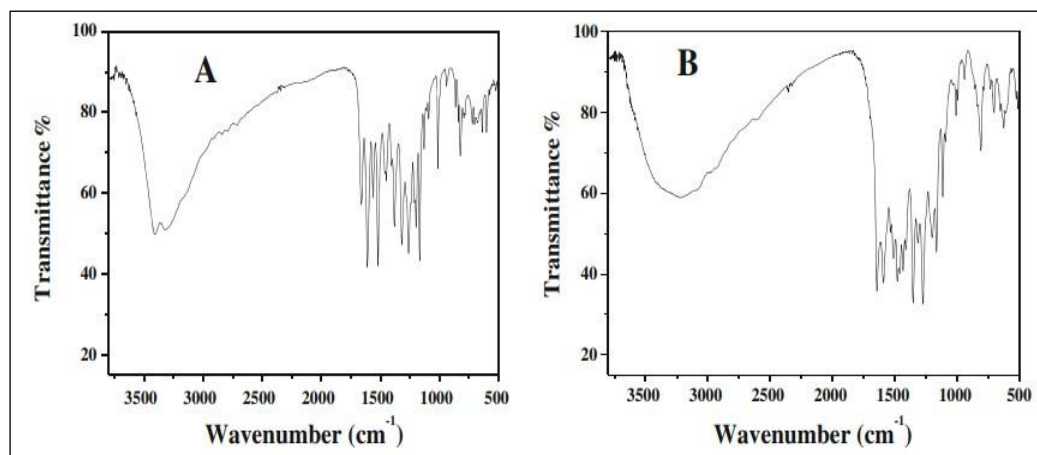


Figure 2.6 The IR spectra of quercetin (A) and Fe(II)-quercetin complex (B)
Source: Raza *et al.* (2016)

A study conducted by da Silva *et al.* (2019) to obtain infrared spectra by producing samples as 1:20 (m/m) KBr pellets (sample: KBr), and the spectra were recorded in the range of 4000 to 400 cm^{-1} using 32 scans and 4 cm^{-1} resolution. The findings of this study on the Infrared region of quercetin and the complexes were shown in **Table 2.4**. It was observed that some changes had occurred on the main bands due to the complexation process. The main changes that occurred mostly was related to the band of carbonyl group $\nu(\text{C}=\text{O})$. The absorption band is shifted to a lower frequency due to a decrease in the absorption of $\text{C}=\text{O}$ bonding (1661 cm^{-1} in free quercetin), while in the complexes, the bands appear from 1647 to 1606 cm^{-1} . The absorbance for $\text{C}-\text{OH}$ in free quercetin was at 1375 cm^{-1} while in the Fe(II)-quercetin and Ni(II)-quercetin complexes, the bands were observed at 1360 and 1367 cm^{-1} respectively. The stretching $\text{C}=\text{O}$ and $\text{C}-\text{OH}$ vibrations were moved toward lower wavenumbers due to the breakdown of the hydrogen bonds in favour of the metal chelation. Additionally, there was a difference in the sequence of the band's binding due to the distortion of the $\text{C}-\text{OH}$ phenol bond (1090 cm^{-1} in the ligand). The bands are seen in the IR spectrum of the metal quercetin complex

in the range 1508–1448 cm^{-1} were ascribed to the asymmetric stretching of the C–O–metal group at the chelating site of the quercetin molecule. The coordination may occur with the 3-OH group. The absorption bands associated with $\nu(\text{M–O})$ are located in the range 410–590 cm^{-1} . The values of $\nu(\text{M–O})$ in the complexes studied were consistent with Hooke's rule, which states that the greater the mass of the metal, the lower the vibration frequency of the O–M bond.

Table 2.4 Infrared spectroscopy data of quercetin and metal(II)-quercetin complexes in KBr pellets

Compound	$\nu(\text{OH})$	$\nu(\text{C=O})$	$\nu(\text{C=C})$	$\nu(\text{C-OH})$	$\nu(\text{C-O-C})$	$\beta(\text{C-OH})$	$\nu(\text{M-O})$
Quercetin	3250	1661	1602	1375	1239	1090	-
Fe(II)-quercetin	3417	1635	1595	1360	1273	1036	522
Ni(II)-quercetin	3403	1639	1606	1367	1268	1089	487

Source: da Silva *et al.* (2019)

The FT-IR spectroscopy of metal complexes with quercetin also has been observed by Kalinowska *et al.* (2016) within the range of 400–4000 cm^{-1} . KBr matrix pellets were used to measure the samples in solid state. The results of the wavenumbers of selected bands from FT-IR spectra of quercetin and Ni(II)-quercetin complex were shown in **Table 2.5**. Referring to **Table 2.5**, bands corresponding to the stretching vibrations of the -OH groups emerged in the spectral region of 3390–3250 cm^{-1} in the free quercetin ligand. At 1672 cm^{-1} , a strong band originating from the C=O stretches in the quercetin molecule was detected. Due to the breakage of hydrogen bonds in favour of metal chelation, the stretching $\nu(\text{OH})$, $\nu(\text{C=O})$, and deforming $\nu(\text{C–OH})$ vibrations were shifted to lower wavenumbers. The formation of metal complexes also affected the electronic charge distribution in the entire molecule

which can be proven by three factors. The first one was the decrease in the wavenumbers of aromatic ring vibrations, followed by the increase in the wavenumbers of $\nu(\text{C-O-C})$, and lastly the metal coordination involved in the catechol group that could be seen in the spectra of complex bands assigned to the $\nu(\text{C-O})$. The coordination of metal involved in the catechol group could be established by the existence of stretching metal-O vibrations at 443 cm^{-1} .

Table 2.5 FT-IR spectra of metal(II)-quercetin complexes

Bands	Quercetin	Ni(II)-quercetin complex
$\nu(\text{OH})$	3390-3250	3390-3250
$\nu(\text{C=O})$	1672	1651
ν ring	1616	1601
ν ring	1512	1503
$\nu(\text{C-O})$ cathecol group	-	-
ν ring	1429	1444
$\nu(\text{C-O})$ cathecol group	-	1421
$\beta(\text{C-OH})$	1362	1346
$\beta(\text{CH})$	1317	1319
$\nu(\text{C-O-C})$	1244	1246
$\beta(\text{OH})$	1211	1210
$\nu(\text{C-CO-C}) + \beta(\text{C-CO-C})$	1165	1167
$\nu(\text{metal-O})$	-	443

Source: Kalinowska *et al.* (2016)

2.4.3 Mass Spectroscopy

In an experiment conducted by Raza *et al.* (2016), the mass spectra of quercetin and compound Fe(II)-quercetin were obtained. When using the positive mode of the quercetin mass spectrum, the peak obtained at m/z 301.10 was correlated with quercetin while the positive mode observed a peak at m/z 658.24 $[\text{Fe}(\text{L})_2]^+$ corresponds to complex Fe(II)-quercetin with the stoichiometry of (metal 1:2

flavonoid). Another study by Liu and Guo (2015) has implemented a full-scan ESI-MS analysis of Fe(II)-quercetin and Ni(II)-quercetin complexes. The scan range was from m/z 50 to 2000 with the unit mass resolution, and the infusion rate was 3 $\mu\text{L}/\text{min}$. 4.8 kV was used as the spray voltage, and the capillary temperature was adjusted to 180 $^{\circ}\text{C}$. Helium was employed as the collision gas in the multiplexed multistage tests, and the mass isolation width was 2.0 Da. The findings were shown in **Figure 2.7**. Two Fe-quercetin complexes were detected, one at m/z 658 and the other at m/z 1012. Based on the molecular weights, it could be concluded that complex A correlated $[(2\text{Q} - \text{H})\text{Fe}]^+$ (Iron 1:2 quercetin), and complex B was correlated with $[(3\text{Q} - 3\text{H})\text{Fe}_2]^+$ (Iron 2:3 quercetin).

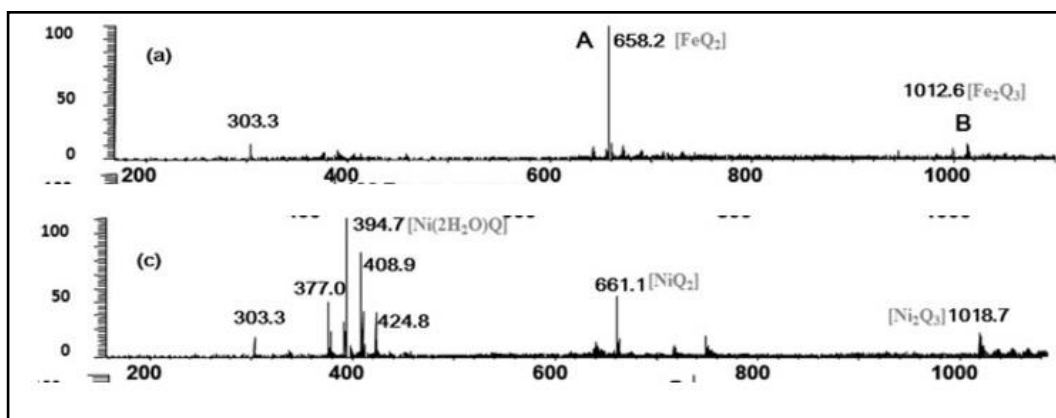


Figure 2.7 Full scan mass spectrum of the Fe(II)-quercetin and Ni(II)-quercetin complexes
Source: Liu and Guo (2015)

Several inferences may be taken from the full-scan mass spectra. Firstly, metal-flavonoid complexes with a stoichiometry of 1:2 and a few complexes with a stoichiometry of 2:3 were produced primarily by Fe(II)-quercetin. Next, a metal-flavonoid complex produced by Ni(II)-quercetin with a stoichiometric of (metal 1:2 flavonoid). In comparison to Ni(II), Fe(II) was easier to synthesize metal-flavonoid complexes due to greater stoichiometric. As a result, it was concluded from this study that the first transition metal ions(II), such as Fe(II) and Ni(II), may form various complexes with quercetin, and that the number of chelating flavonoids reduced as the first transition metal ionic radius decreased (Liu and Guo, 2015). **Table 2.6** shows the reported metal ionic radius, number of d electrons, crystal field stabilisation energies (CFSE), and other variables.

Table 2.6 The ionic radius, number of d electrons and CFSE of the first transition metals

Metal ion	Number of d-electrons	Metal R.	Space Configuration	CFSE(Dq)
Fe(II)	d^6	75 pm	Octahedron	-4
Ni(II)	d^8	70 pm	Octahedron	-12

Source: Liu and Guo (2015)

CHAPTER 3

METHODOLOGY

3.1 Materials

3.1.1 Chemicals

Quercetin dihydrate

Iron(II) sulfate heptahydrate

Nickel(II) chloride hexahydrate

Methanol

Absolute ethanol

Sodium hydroxide

Potassium bromide

Dimethyl sulfoxide-d₆

Boiling chips

3.1.2 Apparatus

50 mL two-necked round-bottomed flask

Electromagnetic stirrer

Magnetic stir plate

Thermometer

Vacuum desiccator

Filter paper

Dropper

Retort stand and clamp

Heating mantle

Reflux condenser

Rubber tubings

Spatula

3.2 Methods

3.2.1 Synthesis of Fe(II) complex with quercetin

A revised technique was used to synthesize Fe(II)-quercetin complex by referring to procedures in Raza *et al.* (2016) and Papan *et al.* (2020). The metal:quercetin compounds were combined in 1:2 mole in 50 cm³ two-necked round-bottomed flask equipped with an electromagnetic stirrer and thermometer. 0.04 mol (0.120 g) of quercetin dissolved into 25 mL of methanol was slowly added with 50 % (w/V) of NaOH solution to adjust the pH to 12. . This process was carried out to alter the protonated quercetin to its deprotonated state. The quercetin solution was mixed with 0.02 mol (0.055 g) Iron(II) sulfate heptahydrate which was pre-dissolved with 10 mL of methanol. Next, the resultant mixture was heated under reflux for six hours at 60 °C and cooled at room temperature. The dark orange precipitates formed were filtered off followed by washing with methanol. Lastly, the final product obtained was dried in a desiccator at room temperature for about 3 days (Kalinowska *et al.*, 2016).

3.2.2 Synthesis of Ni(II) complex with quercetin

A similar technique was used to synthesize Ni(II)-quercetin complex. The metal:quercetin compounds were combined in 1:2 mole in 50 mL two-necked round-bottomed flask equipped with an electromagnetic stirrer and thermometer. 0.04 mol (0.120 g) of quercetin dissolved into 25 mL of methanol was slowly added with 50 % (w/V) of NaOH solution to adjust the pH to 12. . This process was carried out to alter the protonated quercetin to its deprotonated state. Then, the quercetin solution was mixed with 0.02 mol (0.055 g) Nickel(II) chloride hexahydrate which was pre-dissolved with 10 mL of methanol. Next, the resultant mixture was heated under reflux for six hours at 60 °C and cooled at room temperature. The dark orange precipitates formed were filtered off followed by washing with methanol. Lastly, the final product obtained was dried in a desiccator at room temperature for about 3 days.

3.2.3 UV-Vis Spectroscopic Study

UV-Visible spectrophotometer was used to analyze quercetin and metal complexes using a standard 1 cm quartz cell in the range of 250-800 nm. The absorption spectra of free quercetin ligand was expected to have two absorption bands at around 372 nm which represents the cinnamoyl system and 256 nm which represents the

benzoyl system. Compared to the absorption spectra of Fe(II) and Ni(II) complexes with quercetin, the bands obtained were expected to be slightly increased from origin. In other words, the bathochromic shift of the bands was expected to occur. This will prove the combination of the Fe(II) and Ni(II) complexes with quercetin has occurred.

3.2.4 IR Spectroscopic Study

FT-IR spectrometer was used to analyze the binding of quercetin and metal complexes with quercetin by using ATR-FTIR with a spectral range of 4000-400 cm^{-1} . The free quercetin ligand was expected to have an initial $\nu(\text{C}=\text{O})$ stretching mode appeared at around 1661 cm^{-1} , $\nu(\text{C}=\text{C})$ at 1611 cm^{-1} and $\nu(\text{C}-\text{O}-\text{C})$ at 1262 cm^{-1} . Compared to IR spectra of Fe(II) and Ni(II) complexes with quercetin, the $\nu(\text{C}=\text{O})$ and $\nu(\text{C}=\text{C})$ frequencies were expected to shift slightly lower while $\nu(\text{C}-\text{O}-\text{C})$ shifted slightly higher from the initial value. This type of shift will prove that the coordination of carbonyl oxygen with metal complexes has occurred due to complex formation.

CHAPTER 4

RESULTS AND DISCUSSION

4.1 Synthesis of metal complexes with quercetin

4.1.1 Synthesis of Fe(II) complex with quercetin

Fe(II) complex with quercetin was synthesized by using the following method. Firstly, quercetin and $\text{FeSO}_4 \cdot 7\text{H}_2\text{O}$ were combined in a ratio of quercetin 2:1 metal (da Silva *et al.*, 2019). By weighing the solid quercetin at approximately 1.5118 g which is equivalent to 0.005 mole, the solid $\text{FeSO}_4 \cdot 7\text{H}_2\text{O}$ was weighed at 0.6950 g which is equivalent to 0.0025 mole. Then, the solid quercetin and $\text{FeSO}_4 \cdot 7\text{H}_2\text{O}$ were dissolved in 10 mL and 25 mL of methanol respectively by using a 50 mL beaker. At this stage, the quercetin solution was noticed as a yellow solution while $\text{FeSO}_4 \cdot 7\text{H}_2\text{O}$ solution was blue-green in colour. Using 100 mL round bottomed-flask equipped with a magnetic stirrer, both solution of quercetin and $\text{FeSO}_4 \cdot 7\text{H}_2\text{O}$ were mixed until the colour turned dark black. The mixed solution then was refluxed and stirred for 6 hours at 65 °C. After reflux and stirring, the reaction mixture was filtered and the product was evaporated at room temperature. The resulting dark black precipitate was washed with methanol several times to remove

the impurities and unreactive part of the reagent before it was dried in a vacuum desiccator for 2 days (Raza *et al.*, 2016). The percentage yield obtained for Fe(II)-quercetin complex formed was 70.15 % which is quite good.

4.1.2 Synthesis of Ni(II) complex with quercetin

Ni(II) complex with quercetin was synthesized by using the following method. Firstly, quercetin and $\text{NiCl}_2 \cdot 6\text{H}_2\text{O}$ were combined in a ratio of quercetin 2:1 metal (da Silva *et al.*, 2019). By weighing the solid quercetin at approximately 1.5118 g which is equivalent to 0.005 mole, the solid $\text{NiCl}_2 \cdot 6\text{H}_2\text{O}$ was weighed at 0.5942 g which is equivalent to 0.0025 mole. Then, the solid quercetin and $\text{NiCl}_2 \cdot 6\text{H}_2\text{O}$ were dissolved in 10 mL and 25 mL of methanol respectively by using a 50 mL beaker. At this stage, the quercetin solution was noticed as a yellow solution while $\text{NiCl}_2 \cdot 6\text{H}_2\text{O}$ solution was green in colour. Using 100 mL round bottomed-flask equipped with a magnetic stirrer, both solution of quercetin and $\text{NiCl}_2 \cdot 6\text{H}_2\text{O}$ were mixed until the colour turned dark brown. The mixed solution then was refluxed and stirred for 6 hours at 65 °C. After reflux and stirring, the reaction mixture was filtered and the product was evaporated at room temperature. The resulting blackish brown precipitate was washed with methanol several times to remove the impurities and unreactive part of the reagent before it was dried in a vacuum desiccator for 2 days (da Silva *et al.*, 2019). The percentage yield obtained for Ni(II)-quercetin complex formed was 71.09 % which is quite good.

4.2 Characterization of Fe(II) and Ni(II) complexes with quercetin

4.2.1 UV-Vis Spectroscopy

In this study, the concentration of the Fe(II)-quercetin and Ni(II)-quercetin complexes were altered into two parts, the concentrated complexes and the diluted complexes. This was done due to the peaks of the complexes between the range of 300-500 nm cannot be detected when using diluted complexes. Furthermore, in the range of 200-300 nm, a lot of noise presents along with the main peaks when using concentrated complexes, making it hard to observe.

Due to their pigmentation, flavonoid like quercetin exhibits distinct bands of absorption in the UV-VIS area and may be measured using spectrophotometric techniques (Kasprzak *et al.*, 2015). Referring to **Table 4.1**, in the presence of ultrapure water as the solvent, the free quercetin ligand exhibited two absorption bands at 373 nm and 286 nm in the UV spectrum. In quercetin's electronic spectrum, there were two significant absorption bands, one related to the conjugated system between ring B and carbonyl of ring C (cinnamoyl system) and the other related to the conjugated system between ring A and carbonyl of ring C (benzoyl system) (Raza *et al.*, 2016). Band I at 373 nm represents the cinnamoyl system, while band II at 286 nm represents the benzoyl system. For spectra recorded for both Fe(II) and Ni(II) complexes, band I was shifted towards longer wavelengths (bathochromic shift), while band II was shifted towards shorter wavelengths.

After coordinating metal ions, the UV spectra of flavonoids change, displaying a bathochromic (red) shift. According to some authors, a decrease in the HOMO-LUMO gap in the flavonoid molecule rather than a Ligand to Metal Charge Transfer (LMCT) transition is thought to be the cause of the bathochromic shift, while others believe that a strong charge transfer from the flavanoid to the metallic center is to be held responsible. The shift in the energetic state may also have an impact on flavonoids' antioxidant activity, which is often enhanced with the chelation of metal ions (Kasprzak *et al.*, 2015). UV-Vis spectroscopy revealed a bathochromic shift in the absorbance of band I for Fe(II)-quercetin and Ni(II)-quercetin complexes, which may be interpreted by the reaction of the metal with the 3-hydroxyl group of quercetin. This causes an electronic redistribution between the flavonoid molecule and the metal ion, resulting in the formation of an extended π -binder system. The 3-hydroxyl group contains more acidic hydrogen, therefore the 3-OH and 4-oxo groups are the initial coordination sites engaged in the complexation process and impact the band displacement (da Silva *et al.*, 2019). Due to its lower acidity and the spatial obstruction resulting from the initial complexation, the hydroxyl group at position 5 is not engaged in the coordination process (Raza *et al.*, 2016).

After the synthesis of the complexes, distinct peaks were detected at 452 nm (band I) and 275 nm (band II) for Fe(II)-quercetin and 414 nm (band I) and 266 nm (band II) for Ni(II)-quercetin. This demonstrates that complex formation between the metal complexes and quercetin has taken place. Band II changed by around 10-20

nm, but band I moved significantly to a region of approximately 50 nm, indicating metal-quercetin coordination through ring C.

According to the studies done by Cherrak *et al.* (2016), the coordination of quercetin with Fe(II) complex, a band at 438 nm in the electronic spectrum indicates the coordination of the metal with the 3-OH group to the metal center of Fe. For the research on quercetin's coordination with Ni(II) complex, Kalinowska *et al.* (2016) discovered that band I has moved to 426 nm, but Shastrala *et al.* (2021) identified a peak at 415 nm. Compared to this study, the band detected in the electronic spectra of Fe(II)-quercetin and Ni(II)-quercetin emerged at 452 nm and 415 nm respectively, indicating that the coordination of Fe(II) and Ni(II) metal ions with the 3-hydroxy and 4-carbonyl groups, the two potential chelating sites on quercetin.

Table 4.1 Spectroscopy data in the UV-Vis region of the quercetin ligand and the Fe(II)-quercetin and Ni(II)-quercetin complexes in ultrapure water

Quercetin		
Wavelength (nm)	Absorbance	
373	1.3681	
286	1.1509	

Iron(II)-Quercetin		
Wavelength (nm)	Absorbance	
275	2.2965	
258	1.7328	
259	1.0869	
271	0.9218	

Iron(II)-Quercetin concentrated		
Wavelength (nm)	Absorbance	
452	4.9200	
398	4.2804	
418	4.2142	
386	4.0988	

Nickel(II)-Quercetin		
Wavelength (nm)	Absorbance	
266	1.2948	
261	1.1374	
269	0.6132	
262	0.6069	

Nickel(II)-Quercetin concentrated		
Wavelength (nm)	Absorbance	
414	3.2729	
408	3.2148	
403	3.1148	
362	2.8815	

Compound	Band I (nm)	Band II (nm)
Quercetin	373	286
Fe(II)-quercetin	452	275
Ni(II)-quercetin	414	266

4.2.2 FTIR Spectroscopy

A comparative study of the IR spectra of the quercetin molecule and the complexes indicated the presence of the main bands, with some changes resulting from the complexation process as shown in **Table 4.2**. In this IR spectral study, two parts of the wavenumber range were observed separately as there was too much noise in the range of 600-440 cm^{-1} exist in both quercetin and metal-quercetin complexes. The resulted complexes differ most with the band allocated to the carbonyl group $\nu(\text{C}=\text{O})$ (da Silva *et al.*, 2019). The characteristic stretching $\nu(\text{C}=\text{O})$ mode of the quercetin occurred at 1667 cm^{-1} , while due to the formation of Fe(II)-quercetin and Ni(II)-quercetin complexes this band appeared at 1639 cm^{-1} and 1645 cm^{-1} respectively. It can be suggested that the Fe(II) and Ni(II) coordination occurred through the carbonyl oxygen atom and the 3-OH or 5-OH group of the quercetin (Birjees Bukhari *et al.*, 2008).

Broad bands of $\nu(\text{OH})$ vibration frequency at 3272 cm^{-1} in quercetin, 3363 cm^{-1} in Fe(II)-quercetin and 3355 cm^{-1} in Ni(II)-quercetin may be assigned for the presence of water (Raza *et al.*, 2016). The $\nu(\text{C}-\text{OH})$ deformation mode observed at 1377 cm^{-1} in the free quercetin ligand, was shifted to 1365 cm^{-1} in the Fe(II)-quercetin and 1374 cm^{-1} in Ni(II)-quercetin. Due to the dissociation of hydrogen bonds in favour of metal complexation, the stretching $\nu(\text{C}=\text{O})$ and deforming $\nu(\text{C}-$

OH) vibrations were shifted toward lower wavenumbers (Trifunsi & Munteanu, 2018).

The band at 1606 cm^{-1} that was associated with the $\nu(\text{C}=\text{C})$ frequency in free quercetin was also shifted lower to 1571 cm^{-1} in Fe(II)-quercetin and 1561 cm^{-1} in Ni(II)-quercetin due to redistribution of electron density in the benzene ring. Besides, the band related to the $\nu(\text{C}-\text{O}-\text{C})$ frequency at 1242 cm^{-1} in free quercetin ligand was shifted slightly higher to 1266 cm^{-1} and 1318 cm^{-1} in Fe(II)-quercetin and Ni(II)-quercetin complexes respectively upon complexation. This finding indicated an increase in bond order, suggesting the occurrence of metal coordination. The formation of metal complexes also affected the electronic charge distribution in whole molecules, as proven by the increase in wavenumbers of $\nu(\text{C}-\text{O}-\text{C})$, and the presence in the spectra of complex bands assigned to the $\nu(\text{C}-\text{O})$ of the catechol group involved in metal coordination (Kalinowska *et al.*, 2016).

Finally, the existence of stretching $\nu(\text{M}-\text{O})$ vibrations at 519 cm^{-1} for Fe(II)-quercetin and 473 cm^{-1} for Ni(II)-quercetin complexes might also prove the interaction of the metal engaged in the catechol group (Raza *et al.*, 2016). In the studied complexes, the values of $\nu(\text{M}-\text{O})$ followed Hooke's law, which states that the greater the mass of the metal, the lower the vibration frequency of the O-M

bond, where M = Ni(II) has a greater mass than Fe(II) (da Silva *et al.*, 2019). Consequently, the FTIR spectrum data demonstrated the binding between Fe(II) and Ni(II) metal ions with quercetin.

Table 4.2 IR spectra of quercetin, Fe(II)-quercetin and Ni(II)-quercetin complexes

Compound	$\nu(\text{O-H})$ cm^{-1}	$\nu(\text{C=O})$ cm^{-1}	$\nu(\text{C=C})$ cm^{-1}	$\nu(\text{C-OH})$ cm^{-1}	$\nu(\text{C-O-C})$ cm^{-1}	$\nu(\text{M-O})$ cm^{-1}
Quercetin	3272	1667	1606	1377	1242	-
Fe(II)- quercetin	3363	1639	1571	1365	1266	519
Ni(II)- quercetin	3355	1645	1561	1374	1318	473

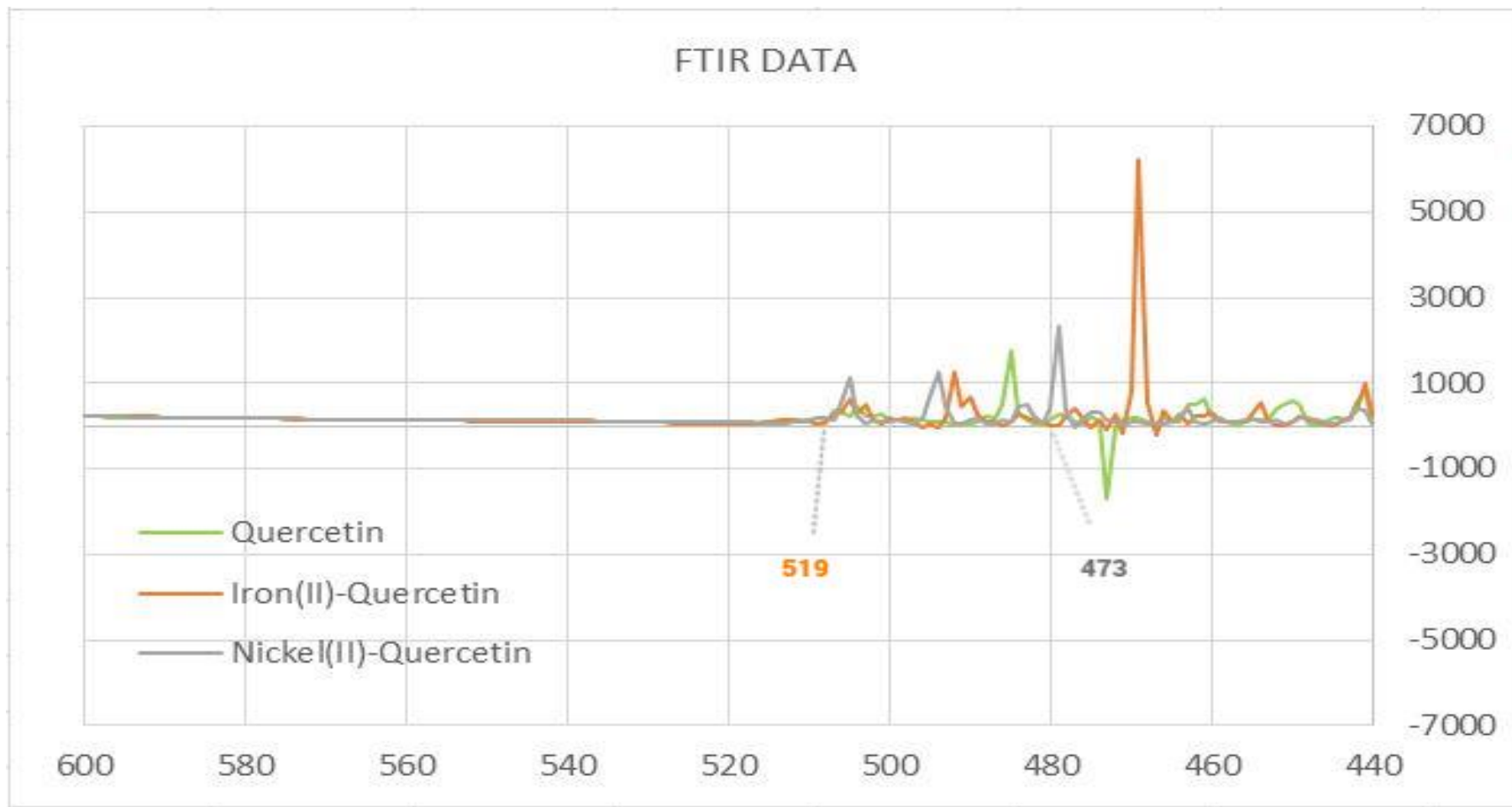


Figure 4.1 FTIR data of quercetin, Fe(II)-quercetin and Ni(II)-quercetin complexes in the range of 600-440 cm^{-1}

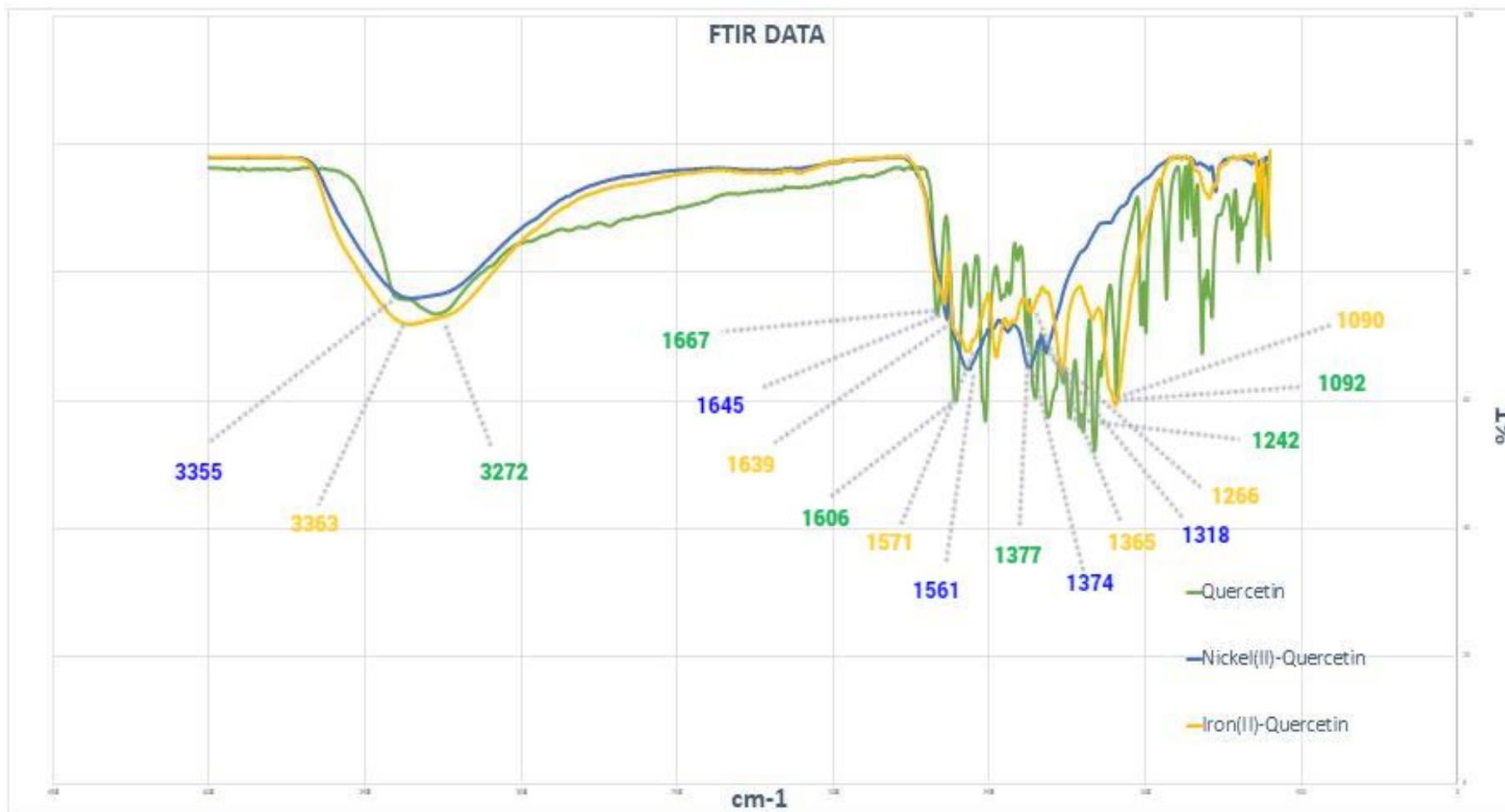


Figure 4.2 FTIR data of quercetin, Fe(II)-quercetin and Ni(II)-quercetin complexes in the range of 4000 – 600 cm⁻¹

CHAPTER 5

CONCLUSION AND RECOMMENDATIONS

5.1 Synthesis and characterization of Fe(II) and Ni(II) complexes with quercetin

The solid commercial quercetin was obtained to undergo complexation with Fe(II) and Ni(II) metal ions. The synthesis of Fe(II) and Ni(II) complexes with quercetin were completed successfully and the project's goal was achieved. The colour of the complexes was dark black for Fe(II)-quercetin while Ni(II)-quercetin was blackish brown. Both complexes were obtained in solid form through the precipitation process and soluble in neither ultrapure water nor distilled water. These complexes were not soluble in any organic solvent such as methanol, ethanol, DMSO, DMF and chloroform. Both Fe(II)-quercetin and Ni(II)-quercetin complexes were obtained to yield a good percentage of 70.15% and 71.09% respectively.

The UV-Vis spectral data displayed evidence of the coordination between metals and quercetin. In the free quercetin ligand, band I which represents the cinnamoyl system was found at 373 nm while band II, the benzoyl system was observed at 286 nm. The band I had experienced a bathochromic shift, shifted towards a longer wavelength (lower energy) when tested with both Fe(II)-quercetin and Ni(II)-quercetin complexes. The new peaks of band I appeared at 452 nm for Fe(II)-quercetin and 414 nm for Ni(II)-quercetin. This result proved that the complexation of metal with quercetin had occurred through 3-hydroxy and 4-carbonyl groups, the two possible chelating sites on quercetin (Liu & Guo, 2015).

The FTIR spectral data also displayed evidence of the coordination between metals and quercetin. The free quercetin ligand showed initial $\nu(\text{C}=\text{O})$ stretching mode appeared at around 1667 cm^{-1} , $\nu(\text{C}=\text{C})$ at 1606 cm^{-1} , $\nu(\text{C}-\text{O}-\text{C})$ at 1242 cm^{-1} , $\nu(\text{C}-\text{OH})$ at 1377 cm^{-1} and $\nu(\text{O}-\text{H})$ at 3272 cm^{-1} . Compared to IR spectra of Fe(II) and Ni(II) complexes with quercetin, the $\nu(\text{C}=\text{O})$, $\nu(\text{C}=\text{C})$, $\nu(\text{C}-\text{OH})$ and $\nu(\text{O}-\text{H})$ frequencies were shifted slightly lower while $\nu(\text{C}-\text{O}-\text{C})$ shifted slightly higher from the initial value. There were also additional spectral data found at 519 cm^{-1} for Fe(II)-quercetin and 473 cm^{-1} for Ni(II)-quercetin which reflected the $\nu(\text{M}-\text{O})$ absorbance. This type of shift proved that the coordination of carbonyl oxygen with metal complexes has occurred due to complex formation (Raza *et al.*, 2016).

5.2 Recommendation

The medical world considers quercetin to be a versatile molecule because of its multiple therapeutic benefits, which include the suppression of carcinogenesis, the decrease of cardiovascular disease, obesity-related illness, cataracts, and neurological disorders (Kazemipour *et al.*, 2018). The biological and pharmacological activities of metal-chelated quercetin are much greater than those of free quercetin ligand (Genckal *et al.*, 2020). Recently, it was shown that flavonoids such as quercetin form high-affinity compounds with transition metal ions such as iron and nickel (Horniblow *et al.*, 2017). This technique is recognized as the main way of enhancing their efficiency in biological functions such as radical scavenging. (Milicevic & Raos, 2016). This study makes suggestions for future research about the development of new metal-quercetin complexes that promote multiple health advantages in the human body. Since these biological activities in the metal-quercetin complex are now in high demand in the medical community, other biological activities including the anti-inflammatory and anticancer effects may be examined in the future. Other physical studies such as thermogravimetric analysis (TGA), differential scanning calorimetry (DSC) and CHNS elemental analysis also may be observed in further studies to support the structure elucidation or identification.

CITED REFERENCES

- Aboo Bakkar, Z., Fulford, J., Gates, P. E., Jackman, S. R., Jones, A. M., Bond, B., & Bowtell, J. L. (2019). Montmorency cherry supplementation attenuates vascular dysfunction induced by prolonged forearm occlusion in overweight, middle-aged men. *Journal of Applied Physiology*, *126*(1), 246-254.
- Bukhari, S. B., Memon, S., Mahroof-Tahir, M., & Bhangar, M. I. (2009). Synthesis, characterization and antioxidant activity copper–quercetin complex. *Spectrochimica Acta Part A: Molecular and Biomolecular Spectroscopy*, *71*(5), 1901-1906.
- Can, M., Armstrong, F. A., & Ragsdale, S. W. (2014). Structure, function, and mechanism of the nickel metalloenzymes, CO dehydrogenase, and acetyl-CoA synthase. *Chemical Reviews*, *114*(8), 4149-4174.
- Cherrak, S. A., Mokhtari-Soulimane, N., Berroukeche, F., Bensenane, B., Cherbonnel, A., Merzouk, H., & Elhabiri, M. (2016). In vitro antioxidant versus metal ion chelating properties of flavonoids: A structure-activity investigation. *PloS one*, *11*(10), e0165575.
- Crans, D. C., & Kostenkova, K. (2020). Open questions on the biological roles of first-row transition metals. *Communications Chemistry*, *3*(1), 1-4.
- da Silva, W. M. B., de Oliveira Pinheiro, S., Alves, D. R., de Menezes, J. E. S. A., Magalhães, F. E. A., Silva, F. C. O., ... & de Moraes, S. M. (2019). Synthesis of quercetin-metal complexes, in vitro and in silico anticholinesterase and antioxidant evaluation, and in vivo toxicological and anxiolytic activities. *Neurotoxicity Research*, 1-11.
- Dávila, Y. A., Sancho, M. I., Almandoz, M. C., & Gasull, E. (2018). Spectroscopic and electronic analysis of chelation reactions of galangin and related flavonoids with nickel (II). *Journal of Chemical & Engineering Data*, *63*(5), 1488-1497.
- De Castilho, T. S., Matias, T. B., Nicolini, K. P., & Nicolini, J. (2018). Study of interaction between metal ions and quercetin. *Food Science and Human Wellness*, *7*(3), 215-219.
- Dixit, R., Malaviya, D., Pandiyan, K., Singh, U. B., Sahu, A., Shukla, R., & Paul, D. (2015). Bioremediation of heavy metals from soil and aquatic environment: an overview of principles and criteria of fundamental processes. *Sustainability*, *7*(2), 2189-2212.
- Fan, D., Alamri, Y., Liu, K., MacAskill, M., Harris, P., Brimble, M., & Guan, J. (2018). Supplementation of blackcurrant anthocyanins increased cyclic

- glycine-proline in the cerebrospinal fluid of parkinson patients: potential treatment to improve insulin-like growth factor-1 function. *Nutrients*, 10(6), 714.
- Gençkal, H. M., Erkisa, M., Alper, P., Sahin, S., Ulukaya, E., & Ari, F. (2020). Mixed ligand complexes of Co (II), Ni (II) and Cu (II) with quercetin and diimine ligands: Synthesis, characterization, anti-cancer and anti-oxidant activity. *JBIC Journal of Biological Inorganic Chemistry*, 25(1), 161-177.
- Grosso, G., Micek, A., Godos, J., Pajak, A., Sciacca, S., Galvano, F., & Giovannucci, E. L. (2017). Dietary flavonoid and lignan intake and mortality in prospective cohort studies: Systematic review and dose-response meta-analysis. *American journal of epidemiology*, 185(12), 1304-1316.
- Gupta, C. P. (2014). Role of iron (Fe) in body. *IOSR Journal of Applied Chemistry*, 7(11), 38-46.
- Hang, Y., Qin, X., Ren, T., & Cao, J. (2018). Baicalin reduces blood lipids and inflammation in patients with coronary artery disease and rheumatoid arthritis: a randomized, double-blind, placebo-controlled trial. *Lipids in health and disease*, 17(1), 1-6.
- Horniblow, R. D., Henesy, D., Iqbal, T. H., & Tselepis, C. (2017). Modulation of iron transport, metabolism and reactive oxygen status by quercetin-iron complexes in vitro. *Molecular nutrition & food research*, 61(3), 1600692.
- Kalinowska, M., Świdorski, G., Matejczyk, M., & Lewandowski, W. (2016). Spectroscopic, thermogravimetric and biological studies of Na (I), Ni (II) and Zn (II) complexes of quercetin. *Journal of Thermal Analysis and Calorimetry*, 126(1), 141-148.
- Kasprzak, M. M., Erxleben, A., & Ochocki, J. (2015). Properties and applications of flavonoid metal complexes. *RSC Advances*, 5(57), 45853-45877.
- Kazemipour, N., Nazifi, S., Poor, M. H. H., Esmailnezhad, Z., Najafabadi, R. E., & Esmaeili, A. (2018). Hepatotoxicity and nephrotoxicity of quercetin, iron oxide nanoparticles, and quercetin conjugated with nanoparticles in rats. *Comparative Clinical Pathology*, 27(6), 1621-1628.
- Kejík, Z., Kaplánek, R., Masařík, M., Babula, P., Matkowski, A., Filipenský, P., & Jakubek, M. (2021). Iron complexes of flavonoids-antioxidant capacity and beyond. *International Journal of Molecular Sciences*, 22(2), 646.
- Khater, M., Ravishankar, D., Greco, F., & Osborn, H. M. (2019). Metal complexes of flavonoids: their synthesis, characterization and enhanced antioxidant and anticancer activities. *Future medicinal chemistry*, 11(21), 2845-2867.

- Koskenkorva-Frank, T. S., Weiss, G., Koppenol, W. H., & Burckhardt, S. (2013). The complex interplay of iron metabolism, reactive oxygen species, and reactive nitrogen species: insights into the potential of various iron therapies to induce oxidative and nitrosative stress. *Free Radical Biology and Medicine*, *65*, 1174-1194.
- Kumar, S., & Trivedi, P. K. (2016). Heavy metal stress signaling in plants. In *Plant Metal Interaction* (pp. 585-603). Elsevier.
- Larson, A. J., Symons, J. D., & Jalili, T. (2012). Therapeutic potential of quercetin to decrease blood pressure: review of efficacy and mechanisms. *Advances in nutrition*, *3*(1), 39-46.
- Liu, Y., & Guo, M. (2015). Studies on transition metal-quercetin complexes using electrospray ionization tandem mass spectrometry. *Molecules*, *20*(5), 8583-8594.
- Luna-Vital, D., Cortez, R., Ongkowijoyo, P., & de Mejia, E. G. (2018). Protection of color and chemical degradation of anthocyanin from purple corn (*Zea mays* L.) by zinc ions and alginate through chemical interaction in a beverage model. *Food Research International*, *105*, 169-177.
- Maitera, O. N., Louis, H., Barminas, J. T., Akakuru, O. U., & Boro, G. (2018). Synthesis and characterization of some metal complexes using herbal flavonoids. *Nat. Prod. Chem. Res*, *6*(314), 10-4172.
- Mathesius, U. (2018). Flavonoid functions in plants and their interactions with other organisms. *Plants*, *7*(2), 30.
- Milicevic, A. (2019). The relationship between antioxidant activity, first electrochemical oxidation potential, and spin population of flavonoid radicals. *Archives of Industrial Hygiene and Toxicology*, *70*(2), 134-140.
- Milicevic, A., & Raos, N. (2016). Modeling of protective mechanism of iron (II)-polyphenol binding with OH-related molecular descriptors. *Croatica Chemica Acta*, *89*(4), 1-6.
- Monk, C., Georgieff, M. K., Xu, D., Hao, X., Bansal, R., Gustafsson, H., & Peterson, B. S. (2016). Maternal prenatal iron status and tissue organization in the neonatal brain. *Pediatric Research*, *79*(3), 482-488.
- Papan, P., Kantapan, J., Sangthong, P., Meepowpan, P., & Dechsupa, N. (2020). Iron (III)-Quercetin Complex: Synthesis, Physicochemical Characterization, and MRI Cell Tracking toward Potential Applications in Regenerative Medicine. *Contrast media & molecular imaging*, 2020.
- Pedro-García, F., Betancourt-Cantera, L. G., Bolarín-Miró, A. M., Cortés-Escobedo, C. A., Barba-Pingarrón, A., & Sánchez-De Jesús, F. (2019).

- Magnetoelectric coupling in multiferroic BiFeO₃ by co-doping with strontium and nickel. *Ceramics International*, 45(8), 10114-10119.
- Pervin, M., Unno, K., Ohishi, T., Tanabe, H., Miyoshi, N., & Nakamura, Y. (2018). Beneficial effects of green tea catechins on neurodegenerative diseases. *Molecules*, 23(6), 1297.
- Peter, A. P., Meersschant, J., Richard, O., Moussa, A., Steenbergen, J., Schaekers, M., & Adelman, C. (2015). Phase formation and morphology of nickel silicide thin films synthesized by catalyzed chemical vapor reaction of nickel with silane. *Chemistry of Materials*, 27(1), 245-254.
- Porkodi, J., & Raman, N. (2018). Synthesis, characterization and biological screening studies of mixed ligand complexes using flavonoids as precursors. *Applied Organometallic Chemistry*, 32(2), e4030.
- Raza, A., Xu, X., Xia, L., Xia, C., Tang, J., & Ouyang, Z. (2016). Quercetin-iron complex: synthesis, characterization, antioxidant, DNA binding, DNA cleavage, and antibacterial activity studies. *Journal of fluorescence*, 26(6), 2023-2031.
- Roy, S., Mallick, S., Chakraborty, T., Ghosh, N., Singh, A. K., Manna, S., & Majumdar, S. (2015). Synthesis, characterisation and antioxidant activity of luteolin–vanadium (II) complex. *Food Chemistry*, 173, 1172-1178.
- Shastrala, K., Kalam, S., Damerakonda, K., Sheshagiri, S. B. B., Kumar, H., Guda, R., ... & Bedada, S. K. (2021). Synthesis, characterization, and pharmacological evaluation of some metal complexes of quercetin as P-gp inhibitors. *Future Journal of Pharmaceutical Sciences*, 7(1), 1-13.
- Silveira, J. Q., Dourado, G. K., & Cesar, T. B. (2015). Red-fleshed sweet orange juice improves the risk factors for metabolic syndrome. *International Journal of Food Sciences and Nutrition*, 66(7), 830-836.
- Singh, T. S., Roy, S. S., Kshetri, P., Ansari, M. A., Sharma, S. K., Verma, M. R., & Kandpal, B. (2021). Comparative study on phenolic, flavonoids and in vitro antioxidant activity of wild edible plants from Loktak Lake wetland ecosystem under North East Indian Himalayan Region. *Natural Product Research*, 35(24), 6045-6048.
- Sivamaruthi, B. S., Kesika, P., & Chaiyasut, C. (2020). The Influence of Supplementation of Anthocyanins on Obesity-Associated Comorbidities: A Concise. *people*, 3, 12-14.
- Tan, S., Wang, C., Lu, C., Zhao, B., Cui, Y., Shi, X., & Ma, X. (2009). Quercetin is able to demethylate the p16INK4a gene promoter. *Chemotherapy*, 55(1), 6-10.

- Trifunsi, S., & Munteanu, M. F. (2018). Synthesis, characterization and antioxidant activity of copper-quercetin complex and iron-quercetin complex. *Rev. Chim.(Bucharest)*, 69.
- Yan, Z., Zhong, Y., Duan, Y., Chen, Q., & Li, F. (2020). Antioxidant mechanism of tea polyphenols and its impact on health benefits. *Animal Nutrition*, 6(2), 115-123.
- Yu, X., Li, Y., & Mu, X. (2020). Effect of quercetin on PC12 Alzheimer's disease cell model induced by A β 25-35 and its mechanism based on sirtuin1/Nrf2/HO-1 pathway. *BioMed Research International*, 2020.
- Zambelli, B., & Ciurli, S. (2013). Nickel and human health. *Interrelations between essential metal ions and human diseases*, 321-357.

CURRICULUM VITAE

A. Personal profile

Full name Muhammad Azrin Bin Md Yusof
National IC no 970814015381
Birth date 14th August 1997
Citizenship MALAYSIA
Place of birth Hospital Sultanah Aminah, Johor Bahru
Gender Male
Correspondence address No. 6, Lrg. 9, Tmn. Seruling Emas, 14200 Sg. Jawi, P. Pinang.
Telephone no. 0196170701
Email address azrxnyusof@gmail.com



B. Hobbies and interests

- Reading and writing
- Photography
- Travelling
- Volunteering at a charity center
- Exploring other cultures

C. Academic qualifications

Degree	Area	Institution	Year
B.Sc. (Hons.)	Chemistry with management	Universiti Teknologi MARA, Malaysia	2022
Diploma	Applied Science	Universiti Teknologi MARA, Malaysia	2019
Sijil Pelajaran Malaysia	Science	Sekolah Menengah Sains Tun Syed Sheh Shahabudin	2014

D. Work Experience

Post	Place	Year
Production operator	Malaysian Automotive Lighting Sdn Bhd, Batu Kawan, Pulau Pinang, Malaysia	2019
Production operator	Seoul Electronic & Telecommunication, Simpang Ampat, Pulau Pinang, Malaysia	2018
Sales promoter	7-eleven, Parit Buntar, Perak, Malaysia	2017
Sales promoter	Yawata Sdn Bhd, Nibong Tebal, Pulau Pinang, Malaysia	2015

E. Related Experience

Post	Place	Year
Participant	Outbound – Inbound Mobility Program	2022
EXCO	Chemists Association, Universiti Teknologi MARA, Malaysia	2020-2021
EXCO	Prismatics Association, Universiti Teknologi MARA, Malaysia	2020-2021
Participant	Modul Kepimpinan Survival Bangsa, Universiti Teknologi MARA, Malaysia	2021
Participant	Online Database For Literature, Universiti Teknologi MARA, Malaysia	2021
Participant	Physician Explorace, Universiti Teknologi MARA, Malaysia	2019
Participant	Modul Pembangunan dan Kepimpinan Pelajar, Universiti Teknologi MARA, Malaysia	2018

F. Awards

Type	Name of award/awarding organisation	Year
Certificate	Dean's List Award 2021, Universiti Teknologi MARA, Malaysia	2022
Certificate	Anugerah Tokoh Akademik Siswa, Universiti Teknologi MARA, Malaysia	2019

G. Skills & Abilities

- Fluent in English and Malay
- Capable in using Microsoft Word, Excel, and Power Point
- Mastered skills in Video and Poster editing: Filmora, Canva, Photoshop and Lightroom
- Capable in using Adobe Animate
- Good teamwork and leadership skill
- Able to work under pressure and multi-task
- Able to follow instructions and deliver quality results
- Have good time management

H. Reference

Madam Rabuyah Ni | Senior Lecturer | +60 16-8767936 | +6082678404